

[illegible]

Report Documentation Page			Form Approved OMB No. 0704-0188		
Public reporting burden for the collection of information is estimated to average 1 hour per response, including the time for reviewing instructions, searching existing data sources, gathering and maintaining the data needed, and completing and reviewing the collection of information. Send comments regarding this burden estimate or any other aspect of this collection of information, including suggestions for reducing this burden, to Washington Headquarters Services, Directorate for Information Operations and Reports, 1215 Jefferson Davis Highway, Suite 1204, Arlington VA 22202-4302. Respondents should be aware that notwithstanding any other provision of law, no person shall be subject to a penalty for failing to comply with a collection of information if it does not display a currently valid OMB control number.					
1. REPORT DATE SEP 2001		2. REPORT TYPE		3. DATES COVERED	
4. TITLE AND SUBTITLE Free-flight aerodynamic characteristic of the LDGP MK-82 CF bomb at subsonic and transonic velocities			5a. CONTRACT NUMBER		
			5b. GRANT NUMBER		
			5c. PROGRAM ELEMENT NUMBER		
6. AUTHOR(S)			5d. PROJECT NUMBER		
			5e. TASK NUMBER		
			5f. WORK UNIT NUMBER		
7. PERFORMING ORGANIZATION NAME(S) AND ADDRESS(ES) Defence R&D Canada - Valcartier, 2459 Pie-XI Blvd North, Quebec (Quebec) G3J 1X5 Canada, ,			8. PERFORMING ORGANIZATION REPORT NUMBER		
9. SPONSORING/MONITORING AGENCY NAME(S) AND ADDRESS(ES)			10. SPONSOR/MONITOR'S ACRONYM(S)		
			11. SPONSOR/MONITOR'S REPORT NUMBER(S)		
12. DISTRIBUTION/AVAILABILITY STATEMENT Approved for public release; distribution unlimited.					
13. SUPPLEMENTARY NOTES					
14. ABSTRACT Free-flight tests were conducted in the Defence Research Establishment Valcartier (DREV) aeroballistic range on a 18.6% scaled model of the Low Drag General Purpose (LDGP) MK82 CF (Conical Fin) bomb from subsonic to low supersonic velocities. All the main aerodynamic coefficients and dynamic stability derivatives, as well as nonlinear ones were determined using the six-degree-of-freedom single- and multiple-fit data reduction techniques. The pitch moment coefficient was highly nonlinear at low angles of attack in the subsonic and transonic regimes. Estimates of the aerodynamic coefficients from three analytical codes and from one computational fluid dynamic analysis were compared with the free-flight results.					
15. SUBJECT TERMS					
16. SECURITY CLASSIFICATION OF:			17. LIMITATION OF ABSTRACT	18. NUMBER OF PAGES 83	19a. NAME OF RESPONSIBLE PERSON
a. REPORT unclassified	b. ABSTRACT unclassified	c. THIS PAGE unclassified			

This page is left blank

This page is left blank

UNCLASSIFIED

DEFENCE RESEARCH ESTABLISHMENT
CENTRE DE RECHERCHES POUR LA DÉFENSE
VALCARTIER, QUÉBEC

DREV - TM - 2001 - 123
Unlimited Distribution / Distribution illimitée

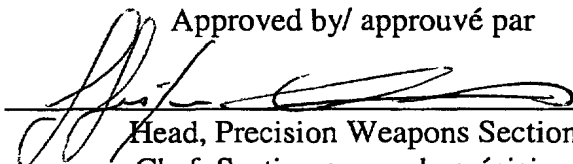
FREE-FLIGHT AERODYNAMIC CHARACTERISTIC OF THE LDGP MK-82 CF
BOMB AT SUBSONIC AND TRANSONIC VELOCITIES

by

A. D. Dupuis

Septembre/septembre 2001

Approved by/ approuvé par


Head, Precision Weapons Section
Chef, Section armes de précision

4 September 2001
Date

SANS CLASSIFICATION

WARNING NOTICE

The information contained herein is proprietary to Her Majesty and is provided to the recipient on the understanding that it will be used for information and evaluation purposes only. Any commercial use, including use for manufacture, is prohibited. Release to third parties of this publication or of information contained herein is prohibited without the prior written consent of DND Canada.

© Her Majesty the Queen in Right of Canada as represented by the Minister of National Defence, 2001

UNCLASSIFIED

i

ABSTRACT

Free-flight tests were conducted in the Defence Research Establishment Valcartier (DREV) aeroballistic range on a 18.6% scaled model of the Low Drag General Purpose (LDGP) MK82 CF (Conical Fin) bomb from subsonic to low supersonic velocities. All the main aerodynamic coefficients and dynamic stability derivatives, as well as nonlinear ones were determined using the six-degree-of-freedom single- and multiple-fit data reduction techniques. The pitch moment coefficient was highly nonlinear at low angles of attack in the subsonic and transonic regimes. Estimates of the aerodynamic coefficients from three analytical codes and from one computational fluid dynamic analysis were compared with the free-flight results.

RÉSUMÉ

Des essais en vol libre ont été effectués dans le corridor aérobalistique du Centre de recherches pour la défense Valcartier (CRDV) avec la bombe, à échelle 18.6%, Low Drag General Purpose (LDGP) MK82 CF (Conical Fin) à des vitesses subsoniques et supersoniques basses. Tous les coefficients aérodynamiques principaux et les dérivés de stabilité dynamique ont été très bien déterminés avec les méthodologies de réduction de six degrés de liberté par les options de réduction simple et multiple. Le coefficient de moment de tangage était très non linéaire à des angles d'attaque peu élevés aux vitesses subsoniques et transsoniques. L'estimation des coefficients aérodynamiques provenant de trois méthodes analytiques, ainsi que d'une analyse des écoulements des fluides a été comparée aux résultats des essais en vol libre.

UNCLASSIFIED
iii

TABLE OF CONTENTS

ABSTRACT/RÉSUMÉ.....i

EXECUTIVE SUMMARYv

NOMENCLATURE.....vii

1.0 INTRODUCTION 1

2.0 MODEL CONFIGURATION3

 2.1 MK82 Configuration3

 2.2 Sabot Design.....6

3.0 FACILITY DESCRIPTION AND TEST CONDITIONS.....7

 3.1 DREV Aeroballistic Range7

 3.3 Test Conditions and Particularities.....8

4.0 FREE-FLIGHT DATA REDUCTION 10

5.0 FREE-FLIGHT RESULTS AND DISCUSSIONS 11

 5.1 Linear Theory Results 11

 5.2 Six-Degree-of-Freedom Results..... 12

 5.3 Comparison of 6DOF Single- and Multiple-Fit Results 14

6.0 AERODYNAMIC PREDICTION METHODOLOGIES..... 17

7.0 COMPARISON OF EXPERIMENTAL AND PREDICTED RESULTS..... 19

 7.1 General Comments22

8.0 CONCLUSIONS AND RECOMMENDATIONS24

9.0 ACKNOWLEDGEMENTS25

10.0 REFERENCES26

TABLES I to VII

FIGURES 1 to 11

APPENDIX A - Angular Motion Plots

UNCLASSIFIED

v

EXECUTIVE SUMMARY

The CF has developed a Store Separation Model (SSM) to predict the separation of stores from the CF-18 aircraft given a configuration and initial conditions. This model was developed in order to reduce the risk of flight test incidents, and to reduce store separation work by directing efforts to critical areas. SSM has been used extensively by Canadair on behalf of DND to support various CF-18 stores clearance projects in the past. The current flight matching technique uses a trial and error approach, which is very time-consuming and costly. It was shown recently that the implementation of the Maximum Likelihood Method (MLM) in the SSM could resolve its inherent deficiencies. The MLM has the capability of extracting aerodynamic coefficients and interference parameters, simultaneously from measured store separation trajectories. The Ballistic SSM (BSSM), under development, would be able to predict full-scale separation and ballistic flight test data for the CF-18 aircraft.

Even though the MLM is a well-proven technique to extract interference coefficients and aerodynamic coefficients (static and dynamic), the store separation tests usually do not have enough angular and translational motion, so that it can be utilized to its maximum efficiency. It is therefore required to have a very good free stream aerodynamic (static and dynamic) coefficient data base of stores dropped from the CF-18 to be able to extract the interference coefficients with a high degree of confidence. If the free stream aerodynamics of the store are in error, the MLM will over or under estimate the interference coefficients to fit the overall observed motion. This reliable free stream aerodynamic data base will also be used with the BSSM to predict accurate store impact at the target and in the CF-18 Ballistic Integrator Algorithm.

DREV has a unique free - flight aeroballistic range where aerodynamic coefficients (static and dynamic) are reduced from measured trajectories with the MLM methodology. Projectiles (scaled or full scale) are fired from a powdered gun through 54 indirect shadowgraph stations. Over the years, this aeroballistic range has shown to be able to extract very reliable aerodynamic coefficients.

DREV was tasked by NDHQ to fire a first series of store configurations in the DREV aeroballistic range with the goal of obtaining their free stream static and dynamic aerodynamic coefficients. The stores that were chosen for this first phase were: LDGP MK82 CF, BDU-5002/B Mod 1 (Modular Practice Bomb - Low Drag), and BDU-5003/B MOD 1 (Modular Practice Bomb - High Drag). The Mach number range of interest is between Mach 0.6 and 1.5.

This memorandum presents the aerodynamic coefficients and stability derivatives that were deduced from free-flight tests conducted in the DREV aeroballistic range on an 18.6% scaled model of the LDGP MK82 CF bomb. All the main aerodynamic coefficients and dynamic stability derivatives as well as nonlinear ones were determined using the six-degree-of-freedom single- and multiple-fit data reduction techniques. The pitch moment coefficient was highly nonlinear at low angles of attack in the subsonic and transonic regimes. The estimates of the aerodynamic coefficients from three analytical codes (PRODAS, AP95 and DATCOM) and from one computational fluid dynamic analysis were compared with the free-flight results.

UNCLASSIFIED

vii

NOMENCLATURE

<u>Variable</u>	<u>Computer Output</u>	<u>Description</u>
A		Cross sectional area of projectile (m^2)
d		Diameter of projectile (mm)
c. g.	CG	Center of gravity (m)
C_{lp}		Roll damping moment coefficient
$C_{l\delta}$		Roll moment coefficient due to fin cant
C_{ly}	Clg	Induced roll moment coefficient
C_{np}	Cnp	Magnus moment coefficient
C_{ny}	Cng	Induced yaw moment coefficient
C_{nsm}	Cnsm	Side moment coefficient
C_N	CN	Normal force coefficient
$C_{N\delta A}$	CNda	Trim force coefficient component
$C_{N\delta B}$	CNdB	Trim force coefficient component
C_M	Cm	Static pitch moment coefficient
C_{Mq}	Cmq	Pitch damping moment coefficient
$C_{M\delta A}$	Cmda	Trim moment coefficient component
$C_{M\delta B}$	CmdB	Trim moment coefficient component
C_{my}	Cmg	Induced pitching moment coefficient
C_{X0}	CX0	Axial force coefficient at zero angle of attack
C_{Yp}	CYp	Magnus moment coefficient
$C_{Y\gamma}$	CYg	Induced normal force coefficient
$C_{Z\gamma}$	CZg	Induced normal force coefficient
I_x, I_y	-	Axial and transverse moments of inertia (kg m^2)

UNCLASSIFIED

viii

l	-	Length of projectile (m)
l/d	-	Length-to-diameter ratio
m	-	Mass of projectile (kg)
M	Mach	Mach number
p	-	Spin rate (rad/s or deg/m)
Re_l	-	Reynolds number based on length of projectile
u, v, w	-	Projectile component velocities (m/s)
V	-	Total projectile velocity (m/s)
X, Y, Z	-	Projectile coordinates (m)
t	-	Time of flight (s)
$\bar{\alpha}$	a	Total angle of attack (deg)
$\bar{\alpha}_{\max}$	AMAX	Maximum angle of attack (deg)
λ_N, λ_P	LN, LP	Nutation and precession damping (1/m)
q, y, f	-	Projectile orientation (deg)
δ	-	Fin cant angle (rad or deg)
δ_T	-	Total trim angle (rad or deg)
$\bar{\delta}^2$	DBSQ	Mean squared yaw (deg ²)
ε	-	Sine of the total angle of attack, $\sin \bar{\alpha} = \frac{v^2 + w^2}{V^2}$
ρ	-	Air density (kg/m ³)
6DOF	-	Six degrees of freedom

UNCLASSIFIED
ix

Subscripts

$\overline{\alpha}_i$	ai (i)	Derivative with respect to ϵ_i
M	M	Variation with Mach number

Examples

$C_{M\overline{\alpha}}$	Cma	Pitching moment coefficient slope
$C_{M\overline{\alpha}^3}$	Cma3	Pitching moment coefficient w.r.t. ϵ^3
$C_{Mq\overline{\alpha}^2}$	Cmq2	Pitch damping coefficient w.r.t. ϵ^2

UNCLASSIFIED

1

1.0 INTRODUCTION

The CF has developed a Store Separation Model (SSM) to predict the separation of stores from the CF-18 aircraft given a configuration and initial conditions in order to reduce the risk of flight test incidents, and to reduce store separation work by directing efforts to critical areas. SSM has been used extensively by Canadair on behalf of DND to support various CF-18 stores clearance projects in the past. Because of inherent model limitations, it is essential to implement the capability to adjust aerodynamic coefficients from the SSM database to match the model predictions with the flight test data. The existing flight matching technique uses an ineffective trial and error approach, which is very time-consuming and costly.

The Defence Research Establishment Valcartier (DREV) has successfully implemented a computerized system which uses the Maximum Likelihood Method (MLM) to iteratively extract aerodynamic coefficients and interference parameters, simultaneously, from the trajectory of test articles in their aeroballistic range and open jet facility. The heart of this system are two computer programs known as the Aeroballistic Range Facility Data Analysis System (ARFDAS, Ref. 1) and Open Jet Facility Data Analysis System (OJFDAS, Ref. 2). OJFDAS, (Ref. 2), successfully showed that it was possible to extract store separation interference coefficients and free stream aerodynamic coefficients (static and dynamic), simultaneously. Feasibility work, which confirmed the compatibility of the MLM algorithms with the SSM, was carried out under MLM Phase 1 efforts (Ref. 3).

A SSM and Ballistic Store Separation Model (BSSM) compatible MLM algorithm, known as the Store Separation Model Data Analysis System (SSMDAS), was tested, under Phase 1 efforts (Ref. 3) and confirmed the ability of MLM techniques to correctly adjust aerodynamic free stream and interference coefficients to match SSM/BSSM predictions to full-scale separation and ballistic flight test data for the CF-18 aircraft. The implementation of such an automated system will improve the accuracy and efficiency of

UNCLASSIFIED

2

DND's SSM and BSSM for future store separation and ballistic work. Canadair has implemented the MLM in the SSM and BSSM (Ref. 4). The modified SSM and BSSM shall have the capability of using MLM techniques to achieve a match of SSM/BSSM predicted trajectories to actual observed separation and free-flight trajectory data of stores dropped from CF-18 aircraft during flight test.

Even though the MLM is a well-proven technique to extract interference coefficients and aerodynamic coefficients (static and dynamic), the store separation tests usually do not have enough angular and translational motion so that it can be utilized to its maximum efficiency. It is therefore required to have a very good free stream aerodynamic (static and dynamic) coefficient database of stores dropped from the CF-18 to be able to extract the interference coefficients with a high degree of confidence. If the free stream aerodynamics of the store are in error, the MLM will over compensate for this, which might lead to errors in the determined interference coefficients. This reliable free stream aerodynamic database will also be used with the BSSM to predict accurate store impact at the target and in the CF-18 Ballistic Integrator Algorithm. An NRC report (Ref. 5) also states this requirement for a reliable aerodynamic data base: "In this component approach to store integration, the essential baseline information is the store free stream aerodynamics. The aircraft flow field, carriage loads, and launch characteristics are considered as interference (not necessarily small) to the aerodynamic characteristic of the store. Hence, whether flight tests, ground tests, or computations are used, a well-established aerodynamic data base for the store itself should be obtained".

DREV has a unique free-flight aeroballistic range (Ref. 6 and 7) where absolute aerodynamic coefficients (static and dynamic) are readily obtainable from measured trajectories with the MLM methodology. Scaled or full-scale projectiles can be fired from a powdered gun through 54 indirect shadowgraph stations. This aeroballistic range has shown over the years to be able to extract very reliable aerodynamic coefficients.

UNCLASSIFIED

3

DREV was tasked by NDHQ to fire a first series of store configurations in the DREV aeroballistic range with the goal of obtaining their free stream static and dynamic aerodynamic coefficients. The stores that were chosen for this first phase were: a scaled LDGP MK-82 CF (18.6%), a full-scale BDU-5002/B Mod 1 (Modular Practice Bomb - Low Drag, MPB - LD) and the BDU-5003/B Mod 1 (Modular Practice Bomb - High Drag, MPB - HD). The Mach number range of interest is between Mach 0.6 and 1.5.

This memorandum presents the aerodynamic coefficients and stability derivatives that were deduced from free-flight tests conducted in the DREV aeroballistic range on an 18.6% scaled model of the LDGP MK82 CF bomb. All the main aerodynamic coefficients and dynamic stability derivatives as well as some nonlinear ones were determined using the six-degree-of-freedom single- and multiple-fit data reduction techniques. The pitch moment coefficient was highly nonlinear at low angles of attack in the subsonic and transonic regime. The estimates of the aerodynamic coefficients from three analytical codes (PRODAS, AP95 and DATCOM) and from one computational fluid dynamic analyses were compared with the free-flight results.

This trials was performed at DREV in October 1998 and the analysis in February 1999, under Work Unit 3ec16, Improvement to CF-18 Ballistics Algorithms.

2.0 MODEL CONFIGURATION

2.1 MK82 Configuration

The LDGP MK82 CF 500 lb low drag general purpose bomb was chosen as one of the configurations since most of the validation and feasibility of using the MLM in the SSM was conducted from this store dropped from the CF-18 and that there was a high interest in obtaining free stream aerodynamic coefficients to as high as Mach 1.5 for operational use. This store is also in the SSM data base and it would be an ideal

UNCLASSIFIED

4

opportunity to verify its free stream aerodynamic coefficients and expand it to the higher Mach numbers. The model to be fired in the aeroballistic range has to be of course a scaled model.

The configuration for the MK-82 was scaled down to the same diameter as the MPB bombs, that is a nominal diameter of 50.8 mm. This implies that the model is a 18.6% scale model. This diameter was also chosen in order to basically have the same sabot design for all the projectiles (Ref. 8). This saved design as well as manufacturing costs.

With guidance from NDHQ, the exact configuration that was modeled was obtained from various drawings supplied by NDHQ and these are:

- | | |
|------------------------|---|
| a. Drawing No. 1380544 | - Bomb Assembly for MK-82 Mod 2 and 3, General Purpose, 500 lb. |
| b. Drawing No. 1380512 | - Fin Assembly, conical, bomb, MK-82, General Purpose, 500 lb. |
| c. Fin | - Mau-93 Tail fin |
| d. Lugs | - MS3314 Suspension Lugs |
| e. Nose Plug | - Continue Ogive shape to a point |

The configuration without the heat blanket was used. The surface imperfections of the real bomb (rivets, screws, etc.) were not retained for the scaled model.

From all of the above drawings and direction from NDHQ, the geometry of the MK-82 that was retained for the free-flight tests is shown in Fig. 1. The dimensions are given in caliber and the reference diameter is 50.8 mm. The detailed drawings are given in Ref. 8. Special care to the design of the model was taken to keep the center of gravity at the same position of the full-scale bomb.

UNCLASSIFIED

5

The general dimensions of the bomb are given in Fig. 1a. Two holes were drilled in line with a pair of fins to be able to launch the projectile with the sabot design (next section). The nominal center of gravity of the projectiles was situated at 3.71 cal from the nose of the projectile. The suspension lugs were located at 45° from a fin. The total length of the projectile is 8.57 cal.

The detailed dimensions of the tail section as well as the fins are shown in Fig. 1b. The fin profile was slightly simplified from the complex fin shape of the full scale bomb. This was done to reduce the manufacturing costs and it is not believed that this will have a major influence on the aerodynamic coefficients. The thickness of the fin was basically kept the same and the angle of cant was retained.

The ogive detail dimensions are provided in Fig. 1c. As mentioned previously, a pointed nose plug was used.

The placements of the suspension lugs and their dimensions were also scaled down and the details are supplied in Fig. 1d. Two small holes of 0.16 cal x 0.16 cal were drilled at 4.87 cal from the base of the projectile so as to be able to fire the scaled model from a sabot. It is not believed that this will affect the aerodynamic performance of the projectile, but special attention for possible shock waves emanating from the holes will be kept when conducting the aeroballistic range tests.

Photographs of the scale MK-82 are shown in Fig. 2. A general view is shown in Fig. 2a. The lug locations as well as the holes are easily seen. An expanded view of the fins is shown in Fig. 2b. A roll pin was added to one of the fins so as to be able to measure the roll orientation of the projectile when conducting tests in the aeroballistic range. The roll pin is placed on the fin situated at -45° from the lug location when viewed from the rear. Figure 2c shows a detailed photograph of the lugs and the holes.

UNCLASSIFIED

6

The nominal physical properties of the models are given in Table I and the physical properties of each test projectile are provided in Table II.

2.2 Sabot Design

Since the subcaliber projectile had to be launched from a powdered gun to conduct tests in the DREV aeroballistic range, special sabots have to be designed to fire them. Since the model configuration in this case is fin stabilized, a smooth bore gun was utilized. The standard gun employed at DREV to fire fin stabilized projectiles of these dimensions in the aeroballistic range is a 110-mm smooth bore gun.

Several aspects have to be considered when designing sabots and models. They are: projectile configuration, total mass, sabot separation at the sabot trap located at 9.2 m from the muzzle at the aeroballistic range, muzzle velocity desired, gun accelerations, etc. The last three mentioned have to be consistent from round to round. In these tests, the highest muzzle velocity desired was approximately 510 m/s (Mach 1.5) and the lowest, 200 m/s (Mach 0.6).

The base area of the MK-82 (Fig. 1) projectile was too small to be able to launch it with a classical pusher type sabot. The launch loads at the highest muzzle velocities would have caused structural failure in that area. It was decided to launch them as the MPB projectiles and use the same launching techniques as the MPBs. For the modular practice bombs the tail portion is made of a polycarbonate material and it is impossible to launch them with a base plate pusher sabot since the projectile would disintegrate at launch. Therefore the modular practice bombs have two locator holes situated close to the center of gravity (Ref.8) and a sabot design that pulls the projectile by these holes is utilized. This launch option saved design as well as manufacturing costs.

UNCLASSIFIED

7

Figure 3 shows a schematic of the sabot for the MK82 scaled projectile. The detail drawings of the sabot are provided in Ref. 8. It is a two-petal sabot design made of aluminum. The lengths of the saw cuts on each side were adjusted to obtain adequate petal separation for the expected velocities. A sabot base seal pad was also used to prevent gas leakage past the sabot body. It has two pins at the front of the sabot to pull the projectile down the barrel. These pins were designed to fit the in service MPB locator holes.

A pivot pin, which is in line with the saw cuts, was added to force the sabot opening at that point. A polycarbonate ring with a 5° angle is positioned at the aft end of the sabot. There are two reasons for this. The first one, is to have a good pressure seal between the sabot and the gun tube so as to be able to have a known shot start pressure which helps in having consistent muzzle velocities at the same propellant charge mass. The second reason is that, as the sabot leaves the gun tube, the high radial pressure acting on the rear ring relative to the front part, causes the pivoting action at the pivot point of the sabot petals.

A photograph of the sabot-model package as well as all the components is shown in Fig. 4. The total model-sabot mass is approximately 4.9 kg.

3.0 FACILITY DESCRIPTION AND TEST CONDITIONS

3.1 DREV Aeroballistic Range

The DREV aeroballistic range (Refs. 6 and 7) is an insulated steel-clad concrete structure used to study the exterior ballistics of various free-flight configurations. The range complex consists of a gun bay, control room and the instrumented range (Fig. 5a). A massive blast wall is located in front of the building to stop sabot pieces and minimize vibrations transmitted to the range structure and instrumentation. Projectiles of calibers

UNCLASSIFIED

8

ranging from 5.56 to 155 mm, including tracer types, may be launched. Large caliber models have been fired up to Mach 7.

The 230-meter instrumented length of the range has a 6.1-m square cross section with a possibility of 54 instrumented sites along the range (Fig. 5b). For most of these tests, 41 of the stations were utilized. These sites house fully instrumented orthogonal shadowgraph stations that yield photographs of the shadow of the projectile as it flies down the range. The maximum shadowgraph window, an imaginary circle within which a projectile will cast a shadow on both reflective screens, is 1.6 meters in diameter. There are also four Schlieren stations (two operational for these tests) at the beginning of the range that yield high quality flow photographs. The range is also air conditioned to maintain a constant relative humidity of approximately 45%. The nominal operational conditions of the range are 20° C at standard atmospheric conditions. The spark source and reference point locations that were used were deduced from a standard survey. A dynamic calibration was conducted in the X, Y, X, θ and ψ coordinates.

3.2 Test Conditions and Particularities

Twelve (12) projectiles were fired in the aeroballistic range program with the 110 mm smooth bore gun with the HI-LO adapter (Ref. 8). All the projectiles had roll pins. The range conditions for each test projectile at time of firing are indicated in Table III. The muzzle velocities range from a low of 230 m/s (Mach 0.6) to a maximum of 382 m/s (Mach 1.11) which yielded Reynolds number, based on the length of projectile, between 6.35×10^6 and 10.7×10^6 , respectively. The angles of attack ranged from a low of 1.8° to a maximum of 6.0°.

The gun muzzle was situated at a downrange coordinate of approximately 6.32 m in the aeroballistic range coordinate system. Due to the low muzzle velocities, the movable butt was utilized to capture the projectiles before the end of the range. It was

UNCLASSIFIED

9

placed after the 47th shadowgraph stations at approximately 150.0 m. This allowed a possibility of 41 shadowgraph stations, or 115.0 m, to measure data. This butt was used for 10 of the 12 projectiles. The full complement of stations (54) was used for two of the models fired at the highest muzzle velocity.

Due to the length of the models, the total shadow of the projectiles in flight could not be captured on the films. A delay was deliberately set so that at least the base of the model could be seen with certainty. This allowed the reading of the films at the front and back of the fins for calculating the trajectory. It was expected that this would cause some errors in the data reductions due to the small-scale length. It is not believed that this significantly affected the reduced aerodynamic coefficients.

A typical Schlieren photograph showing the complex flow and shock structure of a projectile in flight can be seen in Fig. 6 for shot C09 at Mach 0.98. The wake caused by the lugs is easily discernable. A typical shadowgraph photograph is provided in Fig. 7 for projectile C10 at Mach 1.07.

The numbering scheme to refer to the shots and a particular configuration is as follows. The shot numbers are identified by one letter followed by 6 digits, as for example C981002. The letter corresponds to a particular configuration. The first four numbers (9810) indicate the date (year and month) that the projectile was fired in the range. The last two digits correspond to the shot number for that particular configuration. For the example given above, the Shot Number corresponds to the second shot of the Model C configuration that was fired in the range in October 1998. For convenience, the shot numbers are usually referred to the letter and the shot number, C04.

UNCLASSIFIED

10

4.0 FREE-FLIGHT DATA REDUCTION

Extraction of the aerodynamic coefficients and stability derivatives is the primary goal in analyzing the trajectories measured in the DREV aeroballistic range. This was done by means of the Aeroballistic Range Facility Data Analysis System (ARFDAS, Ref. 1) described in Fig. 8. These programs incorporate a standard linear theory and a six-degree-of-freedom (6DOF) numerical integration technique. The 6DOF routine incorporates the Maximum Likelihood Method (MLM) to match the theoretical trajectory with the experimentally measured trajectory. The MLM is an iterative procedure that adjusts the aerodynamic coefficients to maximize a likelihood function. The application of this likelihood function eliminates the inherent assumption in least square theory that the magnitude of the measurement noise must be consistent between parameters (irrespective of units). In general, the aerodynamic coefficients are nonlinear functions of angle of attack, Mach number and roll angle.

ARFDAS represents a complete ballistic range data reduction system capable of analyzing both symmetric and asymmetric models. The essential steps of the data reduction system are to (1) assemble the dynamic data (time, position, angles), model measured physical properties and atmospheric conditions, (2) perform linear theory analysis, and (3) perform 6DOF analysis.

These three steps have been integrated into the data analysis system to provide the test scientist with a convenient and efficient means of interaction. At each step in the analysis, permanent records for each shot are maintained so that subsequent analyses with data modification are much faster.

The 6DOF data reduction system can also simultaneously fit multiple data sets (up to five) to a common set of aerodynamics. Using this multiple-fit approach, a more complete range of angle of attack and roll orientation combinations is available for analysis than would be available from a single flight. This increases the accuracy of the

UNCLASSIFIED

11

determined aerodynamic coefficients over the entire range of angles of attack and roll orientations.

The aerodynamic data presented in this report were obtained using the fixed-plane 6DOF analysis (MLMFXPL) with both the single- and multiple-fit data correlation techniques. The equations of motion have been derived in a fixed-plane coordinate system with Coriolis effects included. The formal derivation of the fixed-plane model is given in Ref. 9.

All the results given here were reduced after the dynamic calibration biases were accounted for the X , Y , X , θ and ψ coordinates. The methodology of the dynamic calibration for the DREV aeroballistic range is explained in Ref. 10.

5.0 FREE-FLIGHT RESULTS AND DISCUSSIONS

The aerodynamic coefficients and stability derivatives that were reduced from the free-flight trajectories measured in the aeroballistic range are presented in tabular form for the linear theory analysis and in both tabular and plotted format for the 6DOF reductions. All of the determined aerodynamic coefficients are given at the mid range measured Mach number.

5.1 Linear Theory Results

The linear theory parameters deduced from the decoupled motion are provided in Table IV. The magnitudes of the angles of attack varied from a low of 1.8° to a high of roughly 5.7° . The amplitude of the initial nutation and precession arms, K_F and K_S , and the mean squared yaw (Db_{sq}) provides an indication of these angles of attack.

UNCLASSIFIED

12

In most cases the shots were dynamically stable as observed by the negative nutation and precession damping modes (LF and LS). Two shots (C04 and C05) show positive nutation damping arms. The frequencies (WF and WS) are consistent. It should be noted that the trim angles (KT) are quite appreciable, of the order of 1.5° . This was expected due to the lugs on the bomb that disturbed the flow.

The aerodynamic coefficients deduced from the linear theory parameters are presented in Table V. The methodology to obtain the aerodynamic coefficients is explained in Ref. 1. The main aerodynamic coefficients (C_{X0} , $C_{N\alpha}$, $C_{M\alpha}$, C_{lp} and $C_{l\delta\delta}$) are consistent. There is some variation in C_{Mq} and this occurs mostly when the angles of attack were quite low, and this is expected in these cases. All the models were statically and dynamically stable, as shown by the negative sign of the pitching moment coefficient slope and the pitch damping coefficient.

The standard deviation error in the angular motion (E-Ang) from the linear theory analysis (Table V) is quite high in some cases. This suggests that the linear theory analysis was not fitting some parameters adequately, probably due to nonlinear variation with angle of attack in some aerodynamic coefficients. These nonlinearities, if they exist, are best modeled and reduced with the 6DOF reduction technique of the next section.

5.2 Six-Degree-of-Freedom Results

The determined aerodynamic coefficients, their standard deviation errors, and the standard deviation errors between the theoretical and experimental trajectories for the axial, angular and roll motions are given in Table VI and Table VII for the single- and multiple-fit data reduction techniques, respectively. The moment reference center for the pitch and moment coefficients was at 43.3% of the length from the nose of the projectile (3.71 cal). All the results are given at the mid-range Mach number for the single-fit data

UNCLASSIFIED

13

reductions and at the average mid-range Mach numbers for the multiple-fit data reductions.

A coefficient that appears with a value and a (*) in parentheses directly below, indicates that this coefficient was held constant and one that has a (-) in parentheses indicates that this coefficient was solved for and that the standard deviation error for this coefficient was higher than 100%, that is, it does not influence the fit and it is considered undetermined. Those with numbers in parentheses represent the standard deviation error for that particular coefficient.

The multiple fit groups were chosen by Mach numbers and six groups of multiple fit data reductions were conducted, as given in Table VII. In some cases, where five shots were reduced simultaneously, it covered a wider Mach number range, since there were no large Mach number effects, especially at the subsonic regime.

As seen from the Tables VI and VII, all of the main aerodynamic coefficients (C_{X0} , $C_{N\alpha}$, $C_{M\alpha}$, C_{Mq} , and $C_{l\delta}$) were very well determined as indicated by the low probable errors of fits on the coefficients. The roll damping moment, C_{lp} , was not as well determined, due to the absence of significant roll motion. The aerodynamic trims were solved for all the shots due to the presence of the lugs. The cubic pitch moment coefficient expansion term, $C_{M_{\alpha^3}}$, was well determined in the multiple data reductions in the subsonic and transonic regime, even though the angles of attack were quite small. The single fit $C_{M_{\alpha^3}}$ were held constant at the determined multiple fit value. The variation of the pitching moment coefficient slope with Mach number, $C_{M\alpha M}$, was also determined in the transonic region. In most single fit reductions, C_{Mq} was also held constant at the multiple fit value.

UNCLASSIFIED

14

The standard deviation errors of the single and multiple fits are of the order of 0.7 mm in the downrange coordinate, 1.7 mm in the swerve motion, 0.35° in pitch and yaw and of the order of 1.0° in roll. These errors of the fits in pitch and yaw and in the swerve direction are a bit high when compared with other test programs conducted in the DREV aeroballistic range. This is probably due to the special film reading technique that was used, as mentioned previously. The 6DOF probable errors of fits are smaller than the linear theory ones because of the better mathematical modeling of the motion, such as the inclusion of aerodynamic trims, angle of attack dependent terms and variations with Mach number.

5.3 Comparison of 6DOF Single- and Multiple-Fit Results

A comparison of the reduced aerodynamic coefficients from the 6DOF data reductions techniques with the single- and multiple-fit results are given in Figures 9. The single fit data points (AB - SF) are shown as open circles while the multiple fit data reduction results (AB - MF) are given as solid circles. Error bars corresponding the standard deviation of the reduced coefficients are provided for the multiple fit data points.

Appendix A presents, for every test shot, the total angle of attack history with the observed angular motion and the theoretical determined one with the reduced aerodynamic coefficients. The experimental data points (open circles) and the calculated trajectory (continuous line) from the determined coefficients are compared. This allows a verification that the reduced aerodynamic coefficients do fit the experimental trajectory satisfactorily. For every shot, the total angle of attack and the angular motion plots in pitch and yaw are given as a function of the downrange coordinate.

The axial force coefficient at zero angle of attack (C_{X0}) as a function of Mach number is shown in Fig. 9a. The subsonic C_{X0} is of the order of 0.14 with a slight

UNCLASSIFIED

15

increase as the Mach number increases and it is of the order of 0.33 at Mach 1.1. The agreement is excellent between the single and the multiple fits.

$C_{N\alpha}$, the normal coefficient slope, versus Mach number is displayed in Fig. 9b. There is a slight scatter in the single fit results due to some low angle of attack cases. $C_{N\alpha}$ is 3.4 at Mach 0.7 and then rises slightly to roughly 4.0 at Mach 0.8 and then decreases again to 3.4 at Mach 0.95. C_{X0} also shows a similar behavior. $C_{N\alpha}$ rises to about 4.8 at Mach 1.1.

The variation of the pitching moment coefficient slope, $C_{M\alpha}$, and the cubic expansion term $C_{M_{\alpha^3}}$ with Mach number are shown in Fig. 9c and Fig. 9d, respectively. The scatter in the single fit results for $C_{M\alpha}$ is higher than would be expected. This is due to the highly nonlinear behavior of the pitch moment coefficient C_M at low angles of attack. As seen in Table VII, the maximum angle of attack measured was of the order of 5.5° . $C_{M_{\alpha^3}}$ was very well determined in the multiple fits, which indicates that this term has a major influence on the motion. $C_{M\alpha}$ is about -1.8 between Mach 0.6 to 0.80, then decreases significantly towards zero in the Mach number range of 0.8 and 0.95, to then increases to -3.8 at Mach 1.1. In other terms, the MK82 loses quite a margin in static stability as it approaches Mach 1.0. $C_{M_{\alpha^3}}$ is of the order -235.0 at Mach 0.7, -130 between Mach .8 and 0.9. It is zero in the low supersonic regime.

The determined pitch damping coefficient, C_{Mq} , as a function of Mach number is presented in Fig. 9e. The error bars are higher than for the other coefficients, but the main trend can be observed. The higher errors are mostly due to the lack in the number of cycles in the angular data and the relatively low angles of attack. In the subsonic regime, C_{Mq} is about -140.0 and roughly -170.0 at Mach 1.1.

UNCLASSIFIED

16

C_{lp} , the roll damping coefficient, is demonstrated versus Mach number in Fig. 9f. The scatter in the results and the errors are quite high below Mach 1.0, but C_{lp} was well determined at Mach 1.1. The high errors and scatter are due to a lack of adequate roll motion in flight.

The data reduction process solves for a total roll moment coefficient due to fin cant $C_{l\delta} \delta$. This coefficient produces the required moment to impose a roll motion or desired spin rate on the projectile. It is solved individually when conducting multiple fits since it is unique for a particular projectile or fin cant. The coefficient that is usually published is $C_{l\delta}$ and in this case, per radian. $C_{l\delta}$ was calculated with the nominal fin cant angle of 1.5° . The trend of $C_{l\delta}$ with Mach number is offered in Fig. 9g. There is some scatter, and the nominal value is of the order of 0.75 for all the Mach number range tested.

The trim angle due to the lugs was calculated as follows. The total trim is:

$$C_{M\delta} \delta_T = \sqrt{(C_{M\delta} \delta_A)^2 + (C_{M\delta} \delta_B)^2}$$

with the total trim as:

$$\delta_T = \arcsin\left(\frac{C_{M\delta} \delta_T}{C_{M\alpha}}\right)$$

The trend of the total trim angle of attack versus Mach number is shown in Fig. 9h. In the low Mach number of 0.6 to 0.8, it is roughly 1.0° and then rises quickly to 6.0° at Mach 1.0. It is less than 0.5° at Mach 1.1.

UNCLASSIFIED

17

The variation of C_M as a function of the angle of attack for the tested Mach numbers is shown in Fig. 10 for the multiple fit data reductions ($C_{M\alpha}$ and $C_{M\alpha^3}$ from Figs. 9c and 9d). The maximum angles of attack observed in the aeroballistic range were of the order of 5.0° . In two cases, where the multiple fit reductions were conducted on five shots, the C_M data was extrapolated to 10.0° assuming no higher nonlinear expansion terms. It was assumed that C_M remained linear up to 10.0° at Mach 1.10. The extrapolated data will be utilized in Section 7.0 with the prediction codes.

6.0 AERODYNAMIC PREDICTION METHODOLOGIES

For design and evaluation purposes, it is necessary to have dependable tools to be able to predict quickly the aerodynamic performance of various projectile configurations. Also, to evaluate the performance of various weapon systems, 6DOF trajectory simulations are usually required and desirable. This implies that a minimum of aerodynamic coefficients are required and these are: C_{X0} , $C_{N\alpha}$, $C_{M\alpha}$, C_{Mq} , C_{lp} and $C_{l\delta}$. These are usually provided as a function of Mach number.

The aerodynamic database on finned projectiles is quite established. The accessible codes are being updated, as the experimental data becomes available. These tools also have to be constantly validated with reliable experimental data to increase the confidence level when utilizing them. The aerodynamic predictions from three of these analytical codes (PRODAS, DATCOM and AP95) were evaluated in this report. The lugs were not modeled in these cases. Also, a CFD analysis, Euler and Navier-Stokes, was also conducted on the MK82 with the lugs, but it only predicted the values for C_{X0} , $C_{N\alpha}$, $C_{M\alpha}$. A short description of each code is given and the predictions are compared with the experimental results in the next section.

UNCLASSIFIED

18

The first aerodynamic predictions were made using the empirical and analytical techniques and tools from PRODAS (PROjectile Design Analysis System, Ref. 11). PRODAS is an interactive tool used to design and analyze various aspects of a weapon system efficiently and quickly, including projectile (spin and fin stabilized) modeling, mass properties, aerodynamic coefficient estimation, stability analysis, internal ballistics, trajectory simulation and so on. It is an integrated system with a common data base and it was developed using proven methodologies and techniques such that the predicted performance estimates are based in part on prior experimental testing. The aerodynamic predictions were obtained from the stability portion of this program.

The aerodynamic predictions of AP-95 (AeroPrediction code 1995, Ref. 12) and DATCOM (Ref. 13) were also evaluated for this configuration. These two codes calculate static and dynamic aerodynamic coefficients for several classes of asymmetric, wing-body-tail configurations. Its basic methodology is that of component superposition where the body alone, lifting surface alone and interference contributions are summed to obtain the total configuration aerodynamics.

The computational fluid dynamic calculations were conducted in two parts. The first part (Ref. 14) involved carrying out Euler calculations on the MK82 store with attachment lugs. The store, at angles of attack of 0.0° and 5.0° , was meshed under both the + and X configurations of fins. Some computations were also conducted for viscous studies with the MK82 without the lugs. The calculations were conducted at Mach numbers of 0.5, 0.8, 1.1 and 1.5. Estimates for C_X , C_N , C_M were obtained at 0.0° and 5.0° . The slopes were calculated to obtain $C_{N\alpha}$ and $C_{M\alpha}$. A second series of computations were done with a Navier-Stokes code at an angle of attack of 10.0° on the MK82 in the X configurations with the lugs. The same Mach number range as before was retained. The Navier-Stokes computations were done with the NASA/AEDC NPARC code. The details of the code and the computations are provided in Ref. 15. C_X , C_N and

UNCLASSIFIED

19

C_M obtained from this viscous analyses will be compared against the free-flight results and the three analytical predictions, where available.

7.0 COMPARISON OF EXPERIMENTAL AND PREDICTED RESULTS

The aerodynamic predictions from PRODAS, AP-95, DATCOM and the Euler/Navier-Stokes are compared in Fig. 11 with the free-flight determined aerodynamic coefficients. The reference center-of-gravity location of the tested projectiles (3.71 cal from nose) was utilized in the calculations for the aerodynamic moment predictions. The free-flight results from both the single- (AB-SF) and multiple-fit (AB-MF) are provided as well as the error bars on the multiple fit results. It should be noted that not all the semi-empirical analytical tools provided estimates for all the coefficients.

The PRODAS calculations for C_{X0} underestimates the free-flight results by approximately 30% subsonically and it agrees very well at Mach 1.1 (Fig. 11a). The PRODAS trend with Mach number also agrees quite well with the free-flight one. The AP95 C_{X0} is the same as the experimental results between Mach 0.5 and 0.8 but it over predicts them by a large margin at Mach 0.8 and Mach 1.1 by roughly 30%. The DATCOM results over predict the test data over the whole subsonic Mach number range by about 50% and by 10% at Mach 1.1. The CFD results for C_{X0} slightly over predicts the trial data by 8% between Mach 0.6 to Mach 1.1. The CFD result shows an increase in C_{X0} as the Mach number decreases below 0.75.

The comparison for the normal force coefficient slope ($C_{N\alpha}$) is shown in Fig. 11b. The PRODAS and AP-95 approximations are similar and they both overestimate the test $C_{N\alpha}$ by 22% over the whole Mach number range tested. The AP95 Mach number trend below Mach 0.7 is quite different from the PRODAS and experimental one. The

UNCLASSIFIED

20

DATCOM data agrees extremely well with the test data over the Mach number range tested. The $C_{N\alpha}$ from the CFD computations are above the free-flight ones by 15% between Mach 0.6 and 0.90 and it provides the same result as the test data at Mach 1.1.

The $C_{M\alpha}$ comparison versus Mach number is shown in Fig. 11c. It is easily seen that the estimates from all the prediction programs tremendously predict more static stability than the free-flight results. DATCOM is off by a factor of at least two, while the other ones by a factor of 5 to 10 in some cases. The worst cases were PRODAS and AP95 and to a lesser extent the CFD results. Since the DATCOM and CFD predictions for $C_{N\alpha}$ were quite reasonable, this implies that the center of pressure location is very badly predicted by these codes to provide such estimates for $C_{M\alpha}$. Strangely enough, the Mach number trend of AP95 follows the free-flight results quite well and to a lesser extent for DATCOM and the CFD estimates.

A comparison of C_M as a function of angle of attack is provided in Fig. 11d to Fig. 11f at nominal Mach numbers of 0.72, 0.90 and Mach 1.1, respectively. PRODAS does not provide nonlinear estimates for the pitch moment coefficient and therefore it is not included in these assessments. Only the multiple fit results of the five shot groups were included.

The first comparison of C_M at Mach 0.72 (Fig. 11d) does not include the CFD results. AP95 overestimates the static stability over the whole angle of attack range and by roughly 30%. The AP95 shows only a slight nonlinear of C_M variation of with angle of attack. The DATCOM estimates of C_M agree quite well up to 6.0° . There is a sharp discontinuity in the DATCOM data at 4.0° probably due the methodology used in the analysis process. The DATCOM C_M above 4.0° indicates less static stability than the free-flight data and by about 30% at 10.0° .

UNCLASSIFIED

21

The estimates of C_M for the three codes at Mach 0.90 are provided in Fig. 11e. Again, AP95 severely overestimates the free-flight results at all angles of attack and by up to a factor of 2 at 10.0° . The DATCOM results agree quite well with the free-flight data at the higher high angles of attack in this case but over predicts slightly at the lower ones. The CFD Euler point at 5.0° is over the free-flight data by a factor of three while at 10.0° angle of attack it over predicts the free-flight stability by 23%.

The C_M approximations with yaw at Mach 1.1 are compared with the test data in Fig. 11f. The free-flight data in this case is linear, at least up to the observed angles of attack measured in the aeroballistic range. The AP95 data again severely over predicts the static stability over the whole angle of attack range. The Euler data point at 5.0° is the same as the DATCOM result but both are quite a bit higher than the free-flight results. The viscous calculation at 10.0° slight overestimates the free-flight results by roughly 32% while the DATCOM data continues in a slight nonlinear fashion to reach -1.4, that is almost a factor of 3, higher than the experimental data.

There are definitely two trends with the CFD C_M data. The viscous calculations at 10.0° yaw are closer to the free-flight data than the Euler calculations at 5.0° . It would be interesting to conduct viscous calculations at the lower angles of attack, as for example 1.0° , 2.0° , 3.0° , 4.0° and 5.0° since the experimental data for C_M show a highly nonlinear behavior even at the low angles of attack. The CFD results at zero angle of attack did produce a small value of C_M with the same magnitude as the free-flight data.

The pitch damping coefficient, C_{Mq} , comparison is presented in Fig. 11g. There are no CFD results for the dynamic stability derivatives. For this coefficient, PRODAS and AP95 predict more pitch damping than the test data by a factor 2.0 over the whole Mach number range. It should be noted that some AP95 data points are off scale in the Mach number region above 1.3 and in the positive sense. The DATCOM data over predicts the determined pitch damping by 33%. Again the trends with Mach number of

UNCLASSIFIED

22

PRODAS, DATCOM and to some extent, AP95, follow the free-flight results, but the magnitudes are not correct.

The C_{lp} (roll damping coefficient) assessment is shown in Fig. 11h. Up to Mach 1.1, all three analytical codes provide roughly the same estimates, but over calculate the free-data by a factor of about three. In this Mach number range, the trends with Mach number are similar to the free-flight one. AP95 has a sudden jump at Mach 1.2 to -3.5.

Two programs, PRODAS and DATCOM, provided estimates for the roll producing coefficient due to the fin cant, $C_{l\delta}$. The comparison to the free-flight data, Fig. 11i, shows that they slightly overestimate the test data by about 20%, with the right Mach number trend.

7.1 General Comments

It is quite clear from the above that none of the predictive tools used in this analysis provided adequate absolute values for all the aerodynamic coefficients (C_{X0} , $C_{N\alpha}$, $C_{M\alpha}$, C_{Mq} , C_{lp} and $C_{l\delta}$) that would be necessary to conduct reliable 6DOF trajectory simulations, either in the SSM or BSSM models. In some instances, in a particular Mach number range and in an angle of attack scale, the agreement between the estimates and the test data was adequate. Not one particular code can be used to obtain reliable estimates, but a combination of them could be used. This is an easy statement after comparing with the experimental data, but a priori, and without reliable experimental data, it would be very difficult to choose one code that would accomplish the goal, at least for configurations of the MK82 type. There is no doubt, that the CFD calculations did not provide more insight than the three analytical methods, and in fact, it is limited to only static aerodynamic coefficients, namely, C_{X0} , C_N and C_M . CFD could be a very useful

UNCLASSIFIED

23

tool if some static aerodynamic coefficients have a nonlinear behavior with angles of attack.

On the other hand, and in many circumstances, even though the absolute values of the estimates were quite off the experimental data, the trends of the estimated aerodynamic coefficients with Mach number, when compared with the experimental data, were very good. This seems to suggest that an astute combination of free-flight experimental data and the use of the analytical tools could provide a reliable data base of aerodynamic coefficients and stability derivatives that would cover the Mach number and angle of attack range of interest.

The lack of experimental data at Mach 1.5, in this case, was considered to be a deficiency, as this would have allowed a better determination of the Mach number trend at Mach numbers higher than Mach 1.1. It was initially planned to conduct test at this velocity regime, but this sabot design could not be used to launch the MK82 safely at this velocity (Ref. 8). An improved sabot design would be required to launch this type of projectiles at Mach 1.5 and this is planned for future projects. Also, a redistribution of the test Mach numbers, as for example at Mach number of 0.5, 0.9, 1.1 and 1.5, would provide the required test data to obtain the trends of the aerodynamic coefficients with Mach number so that the analytical tools could be used to their maximum efficiency.

The fin cant angle should also be increased to provide more roll to better determine the roll damping and roll producing moment coefficients.

UNCLASSIFIED

24

8.0 CONCLUSIONS AND RECOMMENDATIONS

The aerodynamic characteristics of a 18.6% scaled model of the Low Drag General Purpose (LDGP) MK82 CF (Conical Fin) bomb were determined from free-flight tests conducted in the DREV aeroballistic range. Twelve projectiles were successfully fired in the Mach number range of 0.6 to 1.1. All of the aerodynamic coefficients and stability derivatives (C_{X0} , $C_{N\alpha}$, $C_{M\alpha}$, C_{Mq} , C_{lp} and $C_{l\delta}$) were well determined. The angular motion was dominated by the cubic static moment coefficient term ($C_{M_{\alpha^3}}$) at low angles of attack in the subsonic and transonic regions.

The aerodynamic predictions from three empirical/analytical methodologies (PRODAS, AP95 and DATCOM) as well as from a CFD analysis (Euler and Navier-Stokes) were evaluated. In general, the estimates provided for the MK82 computations were very poor. There is no one individual code that could be used without reliable experimental data. The CFD analysis, limited to only static aerodynamic coefficients, did not provide more dependable estimates than the analytical predictions.

On the other hand, and in many circumstances, even though the absolute values of the estimates were quite off the experimental data, the trends of the estimated aerodynamic coefficients with Mach number, when compared with the experimental data, were very good. This seems to suggest that an astute combination of free-flight experimental data and the use of the analytical tools could provide a reliable data base of aerodynamic coefficients and stability derivatives that would cover the Mach number and angle of attack range of interest. Also, a proper CFD analysis could provide nonlinear variations of some static coefficients with angle of attack.

The lack of experimental data at Mach 1.5 was considered to be a deficiency as this would have allowed a better determination of the Mach number trend at Mach numbers greater than 1.1. A redistribution of the test Mach numbers, Mach numbers of

UNCLASSIFIED

25

0.5, 0.9, 1.1 and 1.5 for example, would provide the required test data to obtain the trends of the aerodynamic coefficients with Mach number so that the analytical tools could be used to their maximum efficiency. Increasing the fin cant angle would also allow a better determination the roll damping and roll producing moment coefficients.

9.0 ACKNOWLEDGEMENTS

The author would like to thank Mrs. L. Audet for the operation of the aeroballistic range during the trials. Also, the perseverance of Mrs. S. Lafond, of SNC IT, in developing, loading and reading the films with such thoroughness is appreciated and shown in the quality of the reduced coefficients. Thanks are also addressed to the whole CEEM-V trials team for their devotion and to Mr. M. Normand of MAETEC in making these tests a success. The predictions from Missile DATCOM conducted by Mr. F. Lesage and the assistance of Mr. W. Hathaway in the data reductions were greatly appreciated.

UNCLASSIFIED

26

10.0 REFERENCES

1. "ARFDAS97", Version 4.11, Arrow Tech Associates Inc, August 1997.
2. "Open Jet Facility Data Analysis System (OJFDAS)", Arrow Tech Associates Inc., DREV Contract No. W7701-0-1227, March 1992.
3. "Development of the MLM with Interference Coefficients and Tabular Aerodynamics for SSMDAS", Arrow Tech Associates, DREV contract No. W7701-5-2059, March 1996
4. Stathopoulos, N. and Ouellet, M., "Implementation of MLM for Store Separation Work - Phase II", Bombardier document MAU-261-213, May 1998
5. Jiang, L-J., "Advances in Aircraft/Store Separation Methodologies", NRC, LTR-A-001, October 1995
6. Drouin, G., Dupuis, A. and Côté, F., "Instrumentation Development and Data Analysis for the DREV Aeroballistic Range", DREV M-2800/87, March 1987, UNCLASSIFIED
7. Dupuis, A. and Drouin, G., "The DREV Aeroballistic Range and Data Analysis System", AIAA Paper No. 88-2017, AIAA 15th Aerodynamic Testing Conference, San Diego, California, 18-20 May, 1988.
8. Dupuis, A. D. and Normand, M., "Sabot Performance for Gun Launched MK82 CF, BDU-5003/B and BDU-5002/B MOD 1 Bombs", DREV-TM-9734, January 1998, UNCLASSIFIED

UNCLASSIFIED

27

9. Hathaway, W. H. and Whyte, R., "Aeroballistic Research Facility Free-Flight Data Analysis using the Maximum Likelihood function", AFATL-TR-79-98, December 1979, UNCLASSIFIED.
10. Whyte, R. and Hathaway, W., "Dynamic Calibration of Spark Aeroballistic Ranges", 44th Aeroballistic Range Association Meeting, 13-17 September., 1993, Munich.
11. "Projectile Design Analysis System (PRODAS), PC Version 3.9", Arrow Tech Associates Inc., 1995.
12. Moore, F. G., McInville, R., M. and Hymer, T., "The 1995 Version of the NSWC Aeroprediction Code: Part I - Summary of New Theoretical Methodology", Naval Surface Weapons Center, NSWCCDD/TR-94/379, February 1995, UNCLASSIFIED
13. Burns, K. A., Deters, K. J., Stoy, S. L., Vukelich, S. R. and Blake, W. B, "Missile Datcom Users Manual - Revision 6/93", WL-TR-93-3043, June 1993, UNCLASSIFIED
14. Xu,. H., Khalid, M. and Sun, Y., "A CFD Study of the MK82 Store", NRC-IAR LM-A-037, February 1998, UNCLASSIFIED
15. Xu,. H., Khalid, M. and Chen, Z., "Additinal Euler/Navier-Stokes Computations on DREV Store MK82 with Attachments Lugs ", Letter from NRC-IAR dated 7 June 1999

UNCLASSIFIED

TABLE I
Nominal physical properties of models

d (mm)	m (g)	I _x (g-cm ²)	I _y (g-cm ²)	l (mm)	CG from nose (% /100)
50.8	2494.7	8047.21	178528.0	435.356	0.433

TABLE II
Physical properties of test projectiles

Model #	d (mm)	l (mm)	CG from nose (mm)	CG from nose/l (-)	CG from nose (cal)	m (g)	I _x (g cm ²)	I _y (g cm ²)
C01	50.80	435.077	187.772	0.43158	3.70	2491.2	8031.4	177816.2
C02	50.83	435.204	187.704	0.43130	3.69	2497.2	8055.0	178786.3
C03	50.81	435.204	187.884	0.43171	3.70	2494.0	8044.7	178547.2
C04	50.79	434.417	187.694	0.43206	3.70	2479.6	7996.7	175958.1
C05	50.82	435.306	187.605	0.43097	3.69	2498.6	8057.4	179176.4
C06	50.81	435.331	187.706	0.43118	3.69	2501.1	8070.4	179498.8
C07	50.80	435.077	187.717	0.43146	3.70	2494.9	8052.3	178744.3
C08	50.79	435.306	187.617	0.43100	3.69	2498.8	8060.6	179317.2
C09	50.80	435.408	187.785	0.43129	3.70	2499.6	8060.0	179303.5
C10	50.80	434.823	187.785	0.43187	3.70	2487.7	8026.6	177267.0
C11	50.80	435.204	187.638	0.43115	3.69	2494.6	8041.5	178161.1
C12	50.79	435.001	187.650	0.43138	3.69	2494.8	8053.1	178716.0

UNCLASSIFIED

TABLE III
Range conditions

Shot Number	No. of Stations	Observed Distance (m)	Pressure (mbar)	Temperature (degrees C)	Relative Humidity %	Air Density (kg/m3)	Speed of Sound (m/sec)	Reynolds Number
C981002	38	115.0	984.88000	20.75	38.0000	1.1674	343.673	.635x10 ⁷
C981001	38	115.0	984.01000	20.89	38.0000	1.1658	343.754	.644x10 ⁷
C981003	38	115.0	983.70000	20.88	39.0000	1.1655	343.751	.694x10 ⁷
C981004	37	110.0	987.28000	21.34	35.0000	1.1679	344.016	.729x10 ⁷
C981005	38	115.0	987.08000	21.20	35.0000	1.1682	343.933	.770x10 ⁷
C981006	35	110.0	986.84000	21.26	35.0000	1.1677	343.973	.809x10 ⁷
C981007	34	110.0	1005.15000	20.79	60.5600	1.1913	343.698	.900x10 ⁷
C981008	35	112.5	1004.23000	20.77	61.2400	1.1903	343.682	.927x10 ⁷
C981009	31	112.5	1003.70000	20.95	38.0000	1.1889	343.788	.959x10 ⁷
C981110	46	209.9	984.00000	20.57	33.0000	1.1671	343.566	1.023x10 ⁷
C981011	36	115.0	988.30000	21.24	35.0000	1.1695	343.959	1.073x10 ⁷
C981112	48	209.9	984.00000	20.74	33.0000	1.1664	343.669	1.071x10 ⁷

TABLE IV
Linear theory analysis parameters

Shot No.	Mach No.	Dbsq deg^2	KF deg	KS deg	LF 1/m	LS 1/m	WF deg/m	WS deg/m	WDF deg/m^2	WDS deg/m^2	KT deg	R-ANG deg
C981002	.661	1.92	1.17	1.63	-.0450	-.0029	5.00	-4.76	.000	.002	1.441	.982
C981001	.672	4.86	3.86	3.48	-.0451	-.0081	2.40	-5.34	.000	.000	1.411	.590
C981003	.724	12.51	3.74	2.54	-.0034	-.0067	5.25	-5.95	.000	.000	.079	.398
C981004	.759	1.06	.84	.99	.0032	-.0251	3.77	.32	.006	-.085	.719	.290
C981005	.801	3.77	1.11	1.40	.0082	-.0099	4.62	-4.99	.000	.000	.535	.389
C981006	.842	2.68	.71	4.26	-.0100	-.0180	4.60	-4.81	.000	.000	1.111	.857
C981007	.919	8.91	2.13	3.35	-.0013	-.0074	4.21	-3.87	-.007	-.014	.526	.396
C981008	.947	2.39	2.16	2.16	-.0121	-.0121	4.71	-4.71	.000	.000	.832	1.049
C981009	.980	9.88	3.78	2.26	-.0060	-.0060	3.15	-4.11	.000	.000	1.245	.721
C981110	1.065	.63	2.26	1.90	-.0146	-.0105	5.86	-6.00	.000	.000	.227	.355
C981011	1.116	5.03	2.54	1.89	-.0044	-.0098	5.72	-5.95	.000	.000	.429	.301
C981112	1.117	1.27	2.42	1.89	-.0107	-.0081	7.49	-6.62	.000	.000	.197	.445

UNCLASSIFIED

TABLE V
Linear theory aerodynamic coefficients

Shot No.	Mach No.	Dbsq deg ²	CX0	CX2	CNa	Cma	Cmq	Cnpa	Cld	Clp	Clpw	E-X m	E-SWR m	E-ANG deg	E-PHI deg
C981002	.661	1.9	.145	1.24	1.95	-2.10	-551.8	.01	.0243	-1.8920	.0000	.0007	.0036	.982	.78
C981001	.672	4.9	.124	1.27	3.52	-1.16	-603.3	.01	.0251	-1.9013	.0000	.0007	.0030	.590	1.37
C981003	.724	12.5	.129	1.40	3.52	-2.84	-98.7	.01	.0277	-1.9452	.0000	.0006	.0012	.398	.92
C981004	.759	1.1	.153	1.49	2.59	-1.59	-239.2	.01	.0190	-.6697	.0000	.0005	.0013	.290	.64
C981005	.801	3.8	.147	1.60	3.08	-2.10	-2.7	.01	.0254	-2.0111	.0000	.0005	.0014	.389	1.47
C981006	.842	2.7	.147	1.93	2.32	-2.02	-316.9	.01	.0221	-.8990	.0000	.0005	.0027	.857	1.00
C981007	.919	8.9	.140	2.69	3.45	-1.59	-80.4	.01	.0256	-1.8685	.0000	.0006	.0012	.396	1.06
C981008	.947	2.4	.157	3.13	3.70	-1.98	-259.5	.01	.0175	.3099	.0000	.0008	.0037	1.049	.72
C981009	.980	9.9	.169	3.52	2.67	-1.16	-124.1	.01	.0255	-2.1803	.0000	.0007	.0022	.721	2.07
C981110	1.065	.6	.315	4.25	4.02	-3.17	-270.3	.01	.0239	-.9049	.0000	.0005	.0017	.355	.64
C981011	1.116	5.0	.320	4.78	3.98	-3.08	-144.7	.01	.0228	-.3534	.0000	.0007	.0011	.301	.88
C981112	1.117	1.3	.332	4.79	4.70	-4.50	-194.6	.01	.0250	-1.1093	.0000	.0007	.0017	.445	.74

UNCLASSIFIED

TABLE VI
Six-degree-of freedom aerodynamic coefficients - Single fits

Shot Number	Mach Number	DBSQ ABARM	CX CX2	CNa CNa3	CYpa Cnpa	Cma Cma3	Cmq Cmq2	CZga3 Cmga3	CYga3 Cnga3	Clga2 Cnsm	Clp Cld	Cnda CndB	Cmδα CmδB	Standard Error	
														X(m) Y-Z(m)	Angle(deg) Roll(deg)
C981002	.661	5.6	.143	3.58	.00	-1.605	-132.0	.0	.0	.00	-.940	.008	-.030	.0004	.347
			(0.%) (3.%)	(*) (5.%)	(*) (5.%)	(*) (5.%)	(*) (5.%)	(*) (5.%)	(*) (5.%)	(*) (5.%)	(*) (13.%)	(90.%) (11.%)	(11.%)		
C981002	.661	3.2	1.2	.0	.0	-235.0	.0	.0	.0	.00	.022	.011	-.016	.0013	.633
			(*) (3.%)	(*) (3.%)	(*) (3.%)	(*) (3.%)	(*) (3.%)	(*) (3.%)	(*) (3.%)	(*) (3.%)	(*) (1.%)	(43.%) (10.%)	(10.%)		
C981001	.672	6.6	.124	3.29	.00	-1.865	-132.0	.0	.0	.00	-.735	.003	-.017	.0006	.295
			(0.%) (2.%)	(*) (2.%)	(*) (2.%)	(*) (2.%)	(*) (2.%)	(*) (2.%)	(*) (2.%)	(*) (2.%)	(*) (28.%)	(-) (10.%)	(10.%)		
C981001	.672	4.6	1.3	.0	.0	-235.0	.0	.0	.0	.00	.022	-.025	-.028	.0010	1.056
			(*) (3.%)	(*) (3.%)	(*) (3.%)	(*) (3.%)	(*) (3.%)	(*) (3.%)	(*) (3.%)	(*) (3.%)	(*) (3.%)	(19.%) (7.%)	(7.%)		
C981003	.724	12.1	.132	3.42	.00	-1.427	-132.0	.0	.0	.00	-.900	.000	-.017	.0005	.363
			(1.%) (2.%)	(*) (2.%)	(*) (2.%)	(*) (2.%)	(*) (2.%)	(*) (2.%)	(*) (2.%)	(*) (2.%)	(*) (2.%)	(-) (23.%)	(23.%)		
C981003	.724	5.7	1.4	.0	.0	-235.0	.0	.0	.0	.00	.025	-.011	-.015	.0013	1.598
			(*) (3.%)	(*) (3.%)	(*) (3.%)	(*) (3.%)	(*) (3.%)	(*) (3.%)	(*) (3.%)	(*) (3.%)	(*) (0.%)	(53.%) (12.%)	(12.%)		
C981004	.760	1.6	.153	3.54	.00	-1.796	-132.0	.0	.0	.00	-.714	-.003	-.023	.0004	.296
			(0.%) (3.%)	(*) (3.%)	(*) (3.%)	(*) (3.%)	(*) (3.%)	(*) (3.%)	(*) (3.%)	(*) (3.%)	(*) (24.%)	(-) (8.%)	(8.%)		
C981004	.760	1.8	1.5	.0	.0	-235.0	.0	.0	.0	.00	.019	.009	-.006	.0010	.672
			(*) (3.%)	(*) (3.%)	(*) (3.%)	(*) (3.%)	(*) (3.%)	(*) (3.%)	(*) (3.%)	(*) (3.%)	(*) (2.%)	(48.%) (44.%)	(44.%)		
C981005	.801	5.2	.146	3.64	.00	-1.519	-132.0	.0	.0	.00	-.700	.017	-.029	.0005	.373
			(0.%) (3.%)	(*) (3.%)	(*) (3.%)	(*) (3.%)	(*) (3.%)	(*) (3.%)	(*) (3.%)	(*) (3.%)	(*) (41.%)	(7.%)	(7.%)		
C981005	.801	3.2	1.6	.0	.0	-235.0	.0	.0	.0	.00	.022	.012	-.008	.0011	.647
			(*) (3.%)	(*) (3.%)	(*) (3.%)	(*) (3.%)	(*) (3.%)	(*) (3.%)	(*) (3.%)	(*) (3.%)	(*) (0.%)	(61.%) (45.%)	(45.%)		
C981006	.842	6.3	.146	3.93	.00	-1.822	-162.4	.0	.0	.00	-.562	-.001	-.027	.0003	.354
			(0.%) (2.%)	(*) (2.%)	(*) (2.%)	(*) (2.%)	(*) (2.%)	(*) (2.%)	(*) (2.%)	(*) (2.%)	(*) (48.%)	(-) (8.%)	(8.%)		
C981006	.842	4.3	1.9	.0	.0	-131.0	.0	.0	.0	.00	.021	.004	-.037	.0010	1.185
			(*) (3.%)	(*) (3.%)	(*) (3.%)	(*) (3.%)	(*) (3.%)	(*) (3.%)	(*) (3.%)	(*) (3.%)	(*) (3.%)	(-) (6.%)	(6.%)		
C981007	.919	9.4	.146	3.56	.00	-1.262	-103.7	.0	.0	.00	-.500	.010	-.023	.0005	.293
			(0.%) (2.%)	(*) (2.%)	(*) (2.%)	(*) (2.%)	(*) (2.%)	(*) (2.%)	(*) (2.%)	(*) (2.%)	(*) (47.%)	(7.%)	(7.%)		
C981007	.919	4.9	2.7	.0	.0	-131.0	.0	.0	.0	.00	.023	-.019	-.026	.0009	1.625
			(*) (3.%)	(*) (3.%)	(*) (3.%)	(*) (3.%)	(*) (3.%)	(*) (3.%)	(*) (3.%)	(*) (3.%)	(*) (1.%)	(26.%) (7.%)	(7.%)		

Mach																Standard Error	
Shot Number	Number	DBSQ ABRM	CX CX2	CNa CNa3	CYpa Cnpa	Cma Cma3	Cmq Cmq2	CZga3 Cmga3	CYga3 Cnga3	Clga2 Cnsm	Clp Clid	Cnda CnDB	Cmde CmDB	X(m) Y-Z(m)	Angle(deg) Roll(deg)		
C981008	.947	4.5 3.6	.153 (1.%) 3.1 (*)	3.48 (3.%) .0 (*)	.00 (*)	-.984 (5.%) -131.0 (*)	-138.0 (*)	.0 (*)	.0 (*)	.00 (*)	-.500 (*)	.007 (-)	-.041 (6.%) -.013 (20.%)	.0007	.400		
C981009	.980	10.4 4.8	.167 (1.%) 3.5 (*)	3.47 (2.%) .0 (*)	.00 (*)	-.597 (6.%) -131.0 (*)	-138.0 (*)	.0 (*)	.0 (*)	.00 (*)	-.500 (*)	.010 (-)	-.045 (8.%) -.042 (9.%)	.0006	.449		
C981110	1.066	1.2 3.0	.316 (0.%) 4.2 (*)	3.89 (7.%) .0 (*)	.00 (*)	-3.442 (2.%) .0 (*)	-185.1 (15.%) (*)	.0 (*)	.0 (*)	.00 (*)	-.906 (2.%) -.024 (0.%)	-.003 (-)	.007 (37.%) .012 (52.%)	.0005	.370		
C981011	1.116	4.4 3.4	.322 (0.%) 4.8 (*)	5.00 (3.%) .0 (*)	.00 (*)	-3.388 (2.%) .0 (*)	-184.2 (13.%) (*)	.0 (*)	.0 (*)	.00 (*)	-1.000 (*)	-.043 (22.%)	.017 (17.%) .028 (12.%)	.0005	.315		
C981112	1.117	1.8 3.3	.332 (0.%) 4.8 (*)	4.63 (4.%) .0 (*)	.00 (*)	-4.030 (2.%) .0 (*)	-167.0 (*)	.0 (*)	.0 (*)	.00 (*)	-1.117 (2.%) -.025 (0.%)	-.003 (-)	.025 (12.%) .011 (22.%)	.0008	.389		

UNCLASSIFIED

TABLE VII
Six-degree-of freedom aerodynamic coefficients - Multiple fits

Shot Numbers	Mach Number	DBSQ ABARM	CX (1.%) (3.%)	CNa CNa3 CNa5	CYpa Cnpa Cnpa3 Cnpa5	Cma Cma3 Cma5	Cmq Cmq2 Cmq4	CZga3 Cmga3 Cmga	CYga3 Cnga3 Cnga5	Clga2 CXga2 Clp	CXM CmaM CnsM	Standard Error	
												X(m) Y-Z(m)	Angle(deg) Roll(deg)
C981002	.686	8.0	.133 (1.%) (3.%)	3.43	.00 (*) (4.%) (8.%)	-1.754 (*) (4.%) (8.%)	-133.6 (8.%)	.0 (*)	.0 (*)	.00 (*)	.12 (*)	.0021	.352
C981003		5.5	1.4 (*) (1.%) (3.%)	.0 (*) (1.%) (3.%)	.0 (*) (1.%) (3.%)	-233.6 (*) (8.%)	.0 (*)	.0 (*)	.0 (*)	.00 (*)	2.50 (*)	.0013	1.097
			.0 (*) (1.%) (3.%)	.0 (*) (1.%) (3.%)	.0 (*) (1.%) (3.%)	.0 (*) (1.%) (3.%)	.0 (*)	.0 (*)	.0 (*)	-1.18 (*) (10.%)	.00 (*)		
C981002	.724	6.0	.139 (1.%) (2.%)	3.47	.00 (*) (4.%) (8.%)	-1.694 (*) (4.%) (8.%)	-131.7 (8.%)	.0 (*)	.0 (*)	.00 (*)	.12 (8.%)	.0019	.346
C981004		5.5	1.4 (*) (1.%) (2.%)	.0 (*) (1.%) (2.%)	.0 (*) (1.%) (2.%)	-234.9 (*) (7.%)	.0 (*)	.0 (*)	.0 (*)	.00 (*)	2.46 (20.%)	.0012	1.017
C981003			.0 (*) (1.%) (2.%)	.0 (*) (1.%) (2.%)	.0 (*) (1.%) (2.%)	.0 (*) (1.%) (2.%)	.0 (*)	.0 (*)	.0 (*)	-.93 (*) (10.%)	.00 (*)		
C981004	.801	4.2	.148 (1.%) (2.%)	3.76	.00 (*) (2.%) (11.%)	-1.814 (*) (2.%) (11.%)	-150.0 (11.%)	.0 (*)	.0 (*)	.00 (*)	-.09 (13.%)	.0006	.346
C981006		4.3	1.9 (*) (1.%) (2.%)	.0 (*) (1.%) (2.%)	.0 (*) (1.%) (2.%)	-132.0 (*) (9.%)	.0 (*)	.0 (*)	.0 (*)	.00 (*)	.00 (*)	.0011	.849
			.0 (*) (1.%) (2.%)	.0 (*) (1.%) (2.%)	.0 (*) (1.%) (2.%)	.0 (*) (1.%) (2.%)	.0 (*)	.0 (*)	.0 (*)	-.45 (*) (24.%)	.00 (*)		
C981005	.898	7.1	.137 (0.%) (1.%)	3.62	.00 (*) (5.%) (8.%)	-1.318 (*) (5.%) (8.%)	-138.1 (8.%)	.0 (*)	.0 (*)	.00 (*)	.34 (5.%)	.0007	.384
C981007		5.0	3.5 (*) (1.%) (2.%)	.0 (*) (1.%) (2.%)	.0 (*) (1.%) (2.%)	-131.1 (*) (9.%)	.0 (*)	.0 (*)	.0 (*)	.00 (*)	7.21 (5.%)	.0012	1.311
C981009			.0 (*) (1.%) (2.%)	.0 (*) (1.%) (2.%)	.0 (*) (1.%) (2.%)	.0 (*) (1.%) (2.%)	.0 (*)	.0 (*)	.0 (*)	-.50 (*) (25.%)	.00 (*)		

UNCLASSIFIED

TABLE VII (continued)

Shot Numbers	Mach Number	DBSQ ABARM	CX CX2 CX4	CNa CNa3 CNa5	CYpa Cnpa Cnpa3	Cma Cma3 Cma5	Cmq Cmq2 Cmq4	CZga3 Cmga Cmga	CYga3 Cnga3 Cnga5	Clga2 CXga2 Clp	CXM CnaM CnsM	Standard Error	
												X(m) Y-Z(m)	Angle(deg) Roll(deg)
C981008	.949	8.0	.154 (1.%)	3.53 (1.%)	.00 (*)	-.872 (6.%)	-127.8 (10.%)	.0 (*)	.0 (*)	.00 (*)	.38 (5.%)	.0006	.378
C981009		5.0	3.8 (13.%)	.0 (*)	.0 (*)	-151.4 (8.%)	.0 (*)	.0 (*)	.0 (*)	.00 (*)	10.83 (8.%)	.0012	1.472
			.0 (*)	.0 (*)	.0 (*)	.0 (*)	.0 (*)	.0 (*)	.0 (*)	-.77 (24.%)	.00 (*)		
C981110	1.100	2.4	.326 (0.%)	4.74 (3.%)	.00 (*)	-3.766 (1.%)	-166.8 (9.%)	.0 (*)	.0 (*)	.00 (*)	.30 (4.%)	.0012	.389
C981011		3.3	4.8 (*)	.0 (*)	.0 (*)	.0 (*)	.0 (*)	.0 (*)	.0 (*)	.00 (*)	.00 (*)	.0017	.936
			.0 (*)	.0 (*)	.0 (*)	.0 (*)	.0 (*)	.0 (*)	.0 (*)	-1.00 (2.%)	.00 (*)		

UNCLASSIFIED

FIGURE 1 - MK-82 geometry for aeroballistic range tests
(all dimensions in caliber)

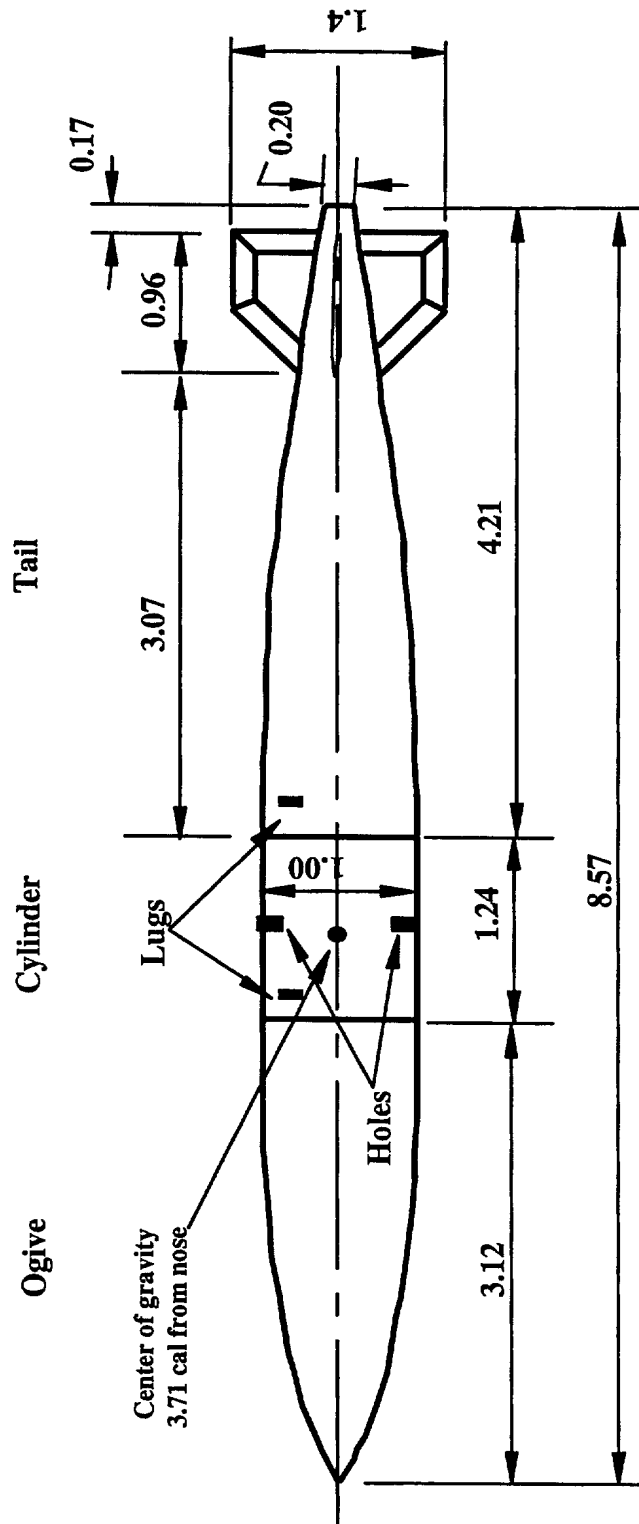


Fig. 1a) General view

UNCLASSIFIED

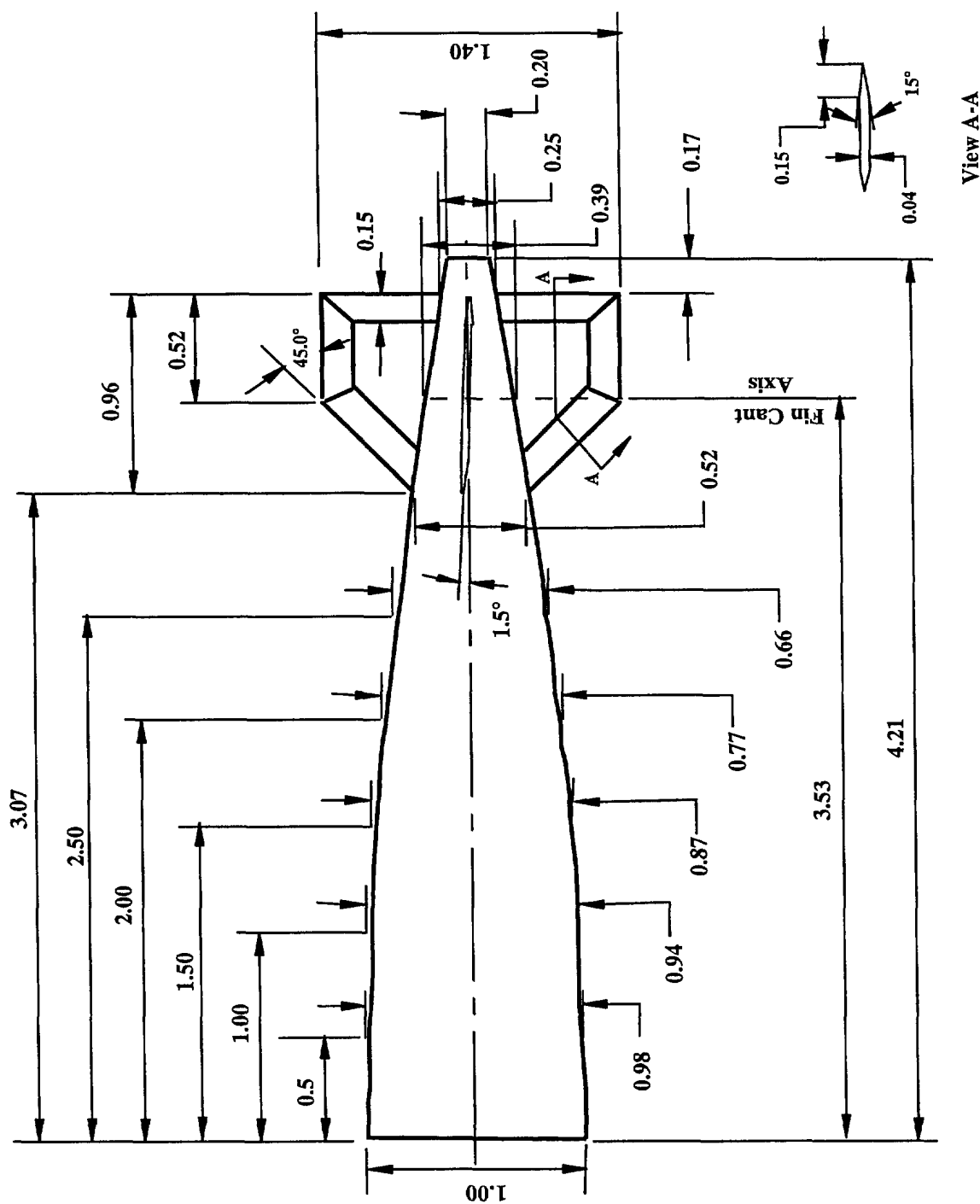


Fig. 1b) Tail and fin details

UNCLASSIFIED

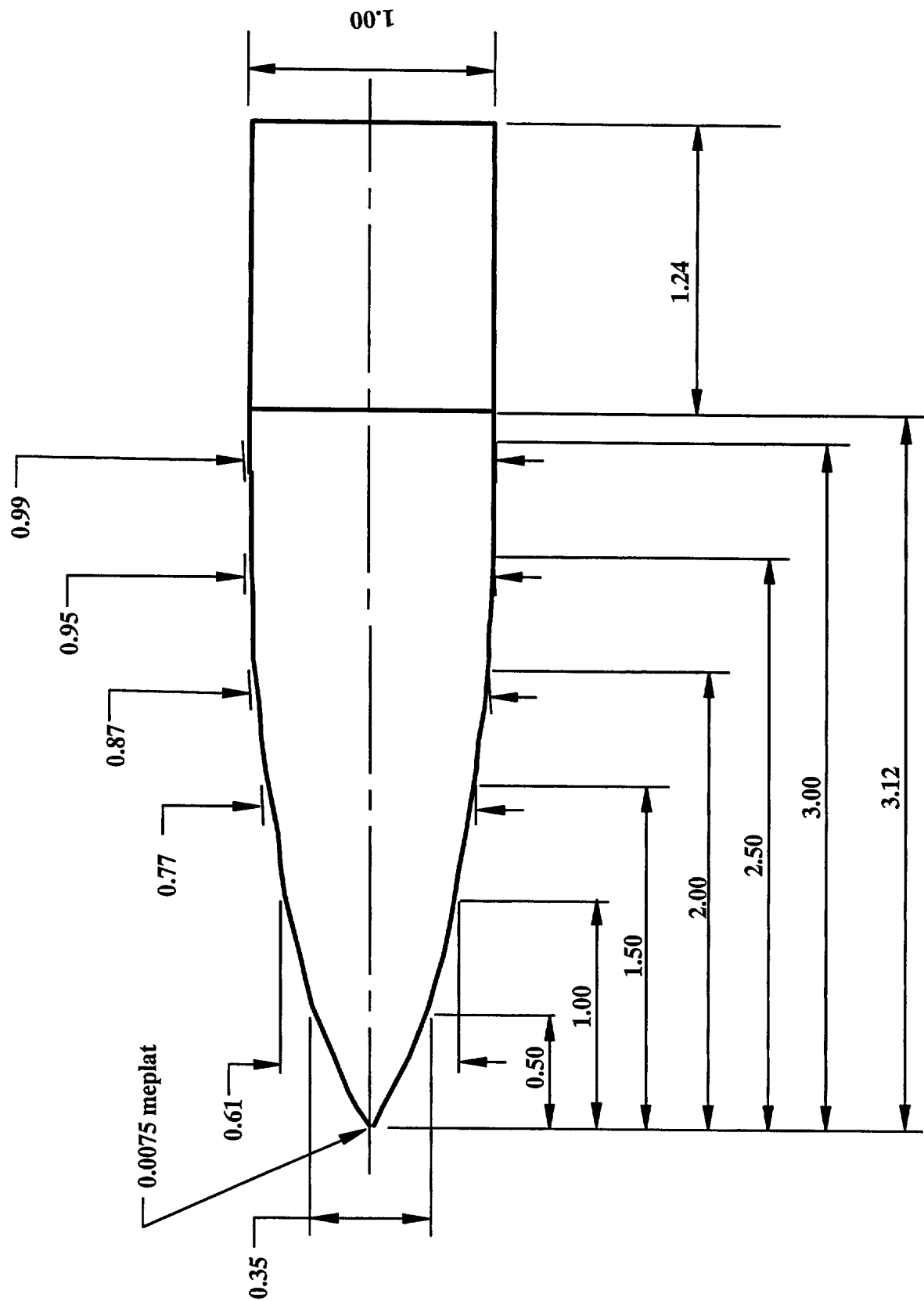
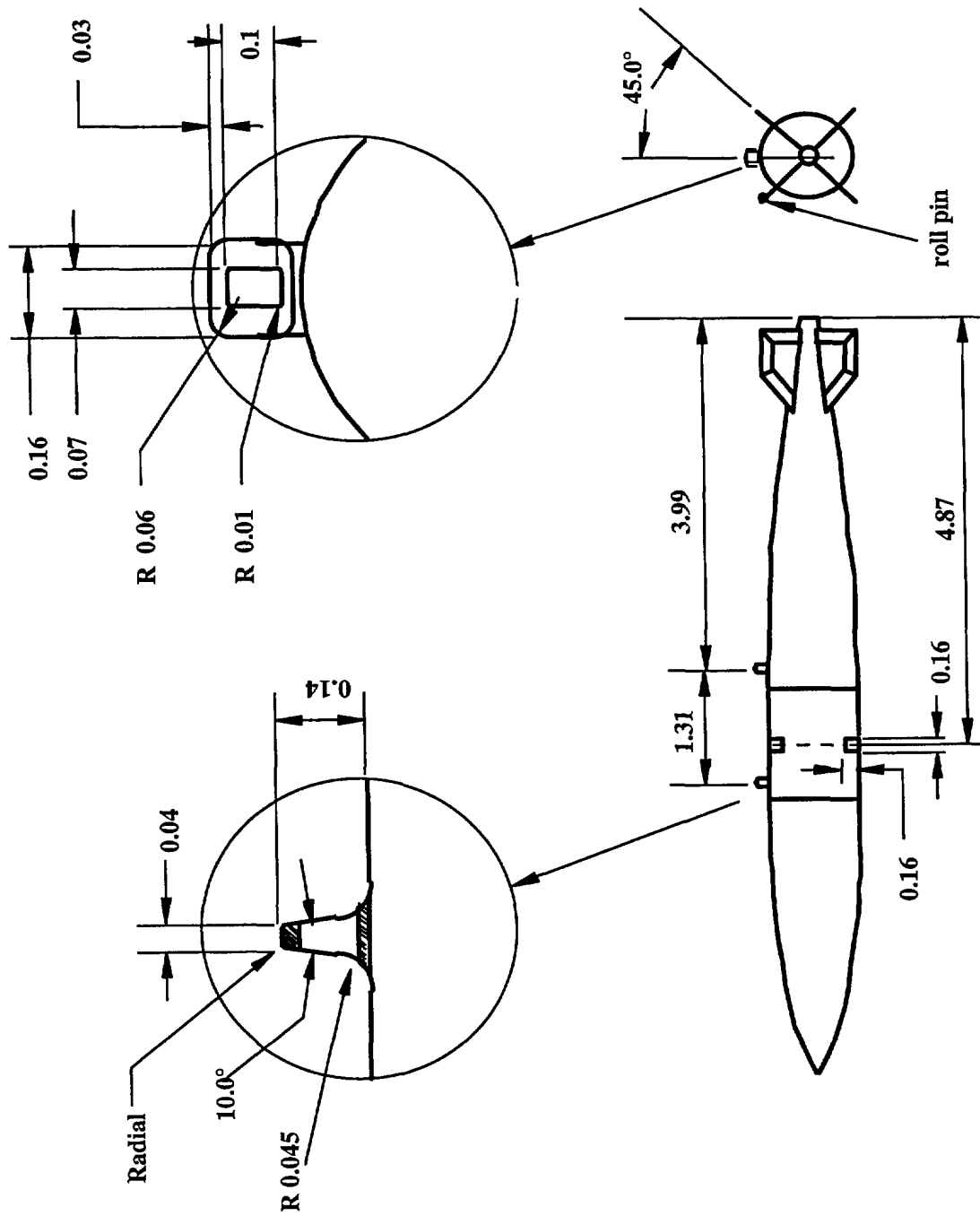


Fig. 1c) Ogive details

UNCLASSIFIED



(Holes drilled in line with fins as per end view)

Fig. 1d) Suspension lugs and sabot pin holes details

UNCLASSIFIED

FIGURE 2- Photographs of scaled free-flight MK-82 projectile

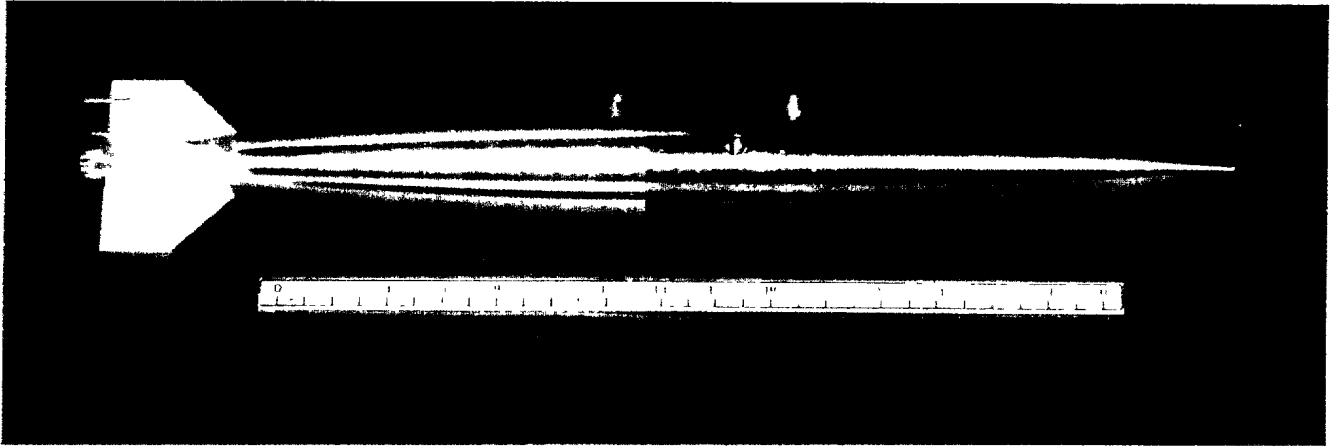


Fig. 2a) General view

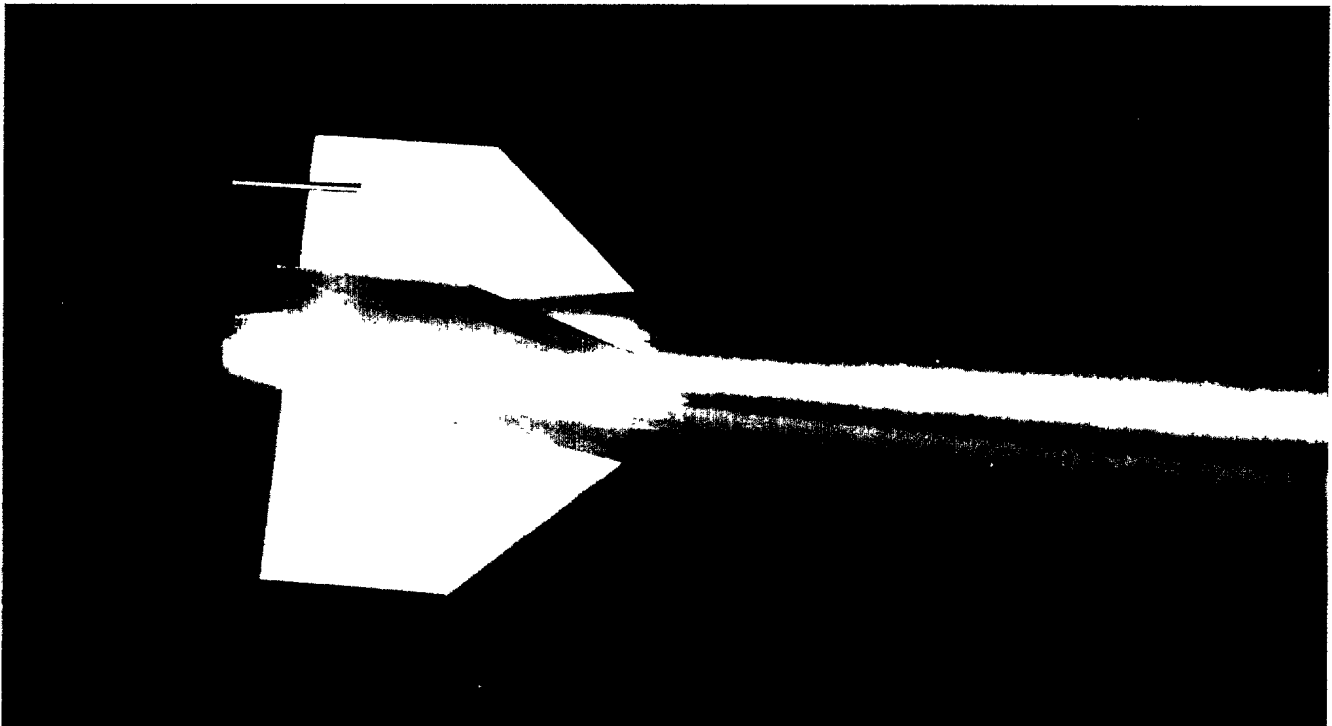


Fig. 2b) Fin detailed view

UNCLASSIFIED



Fig. 2c) Suspension lugs and hole view

UNCLASSIFIED

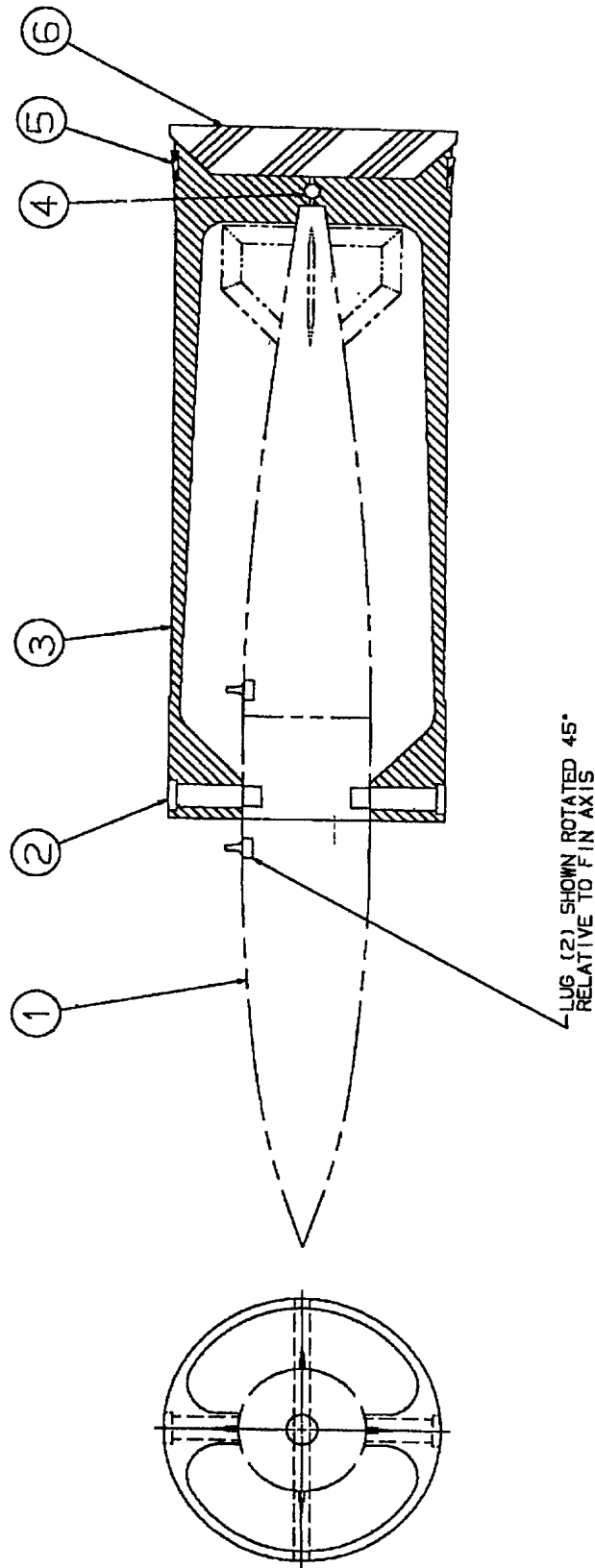


FIGURE 3 - Sabot schematic for the MK-82 scaled projectile

UNCLASSIFIED

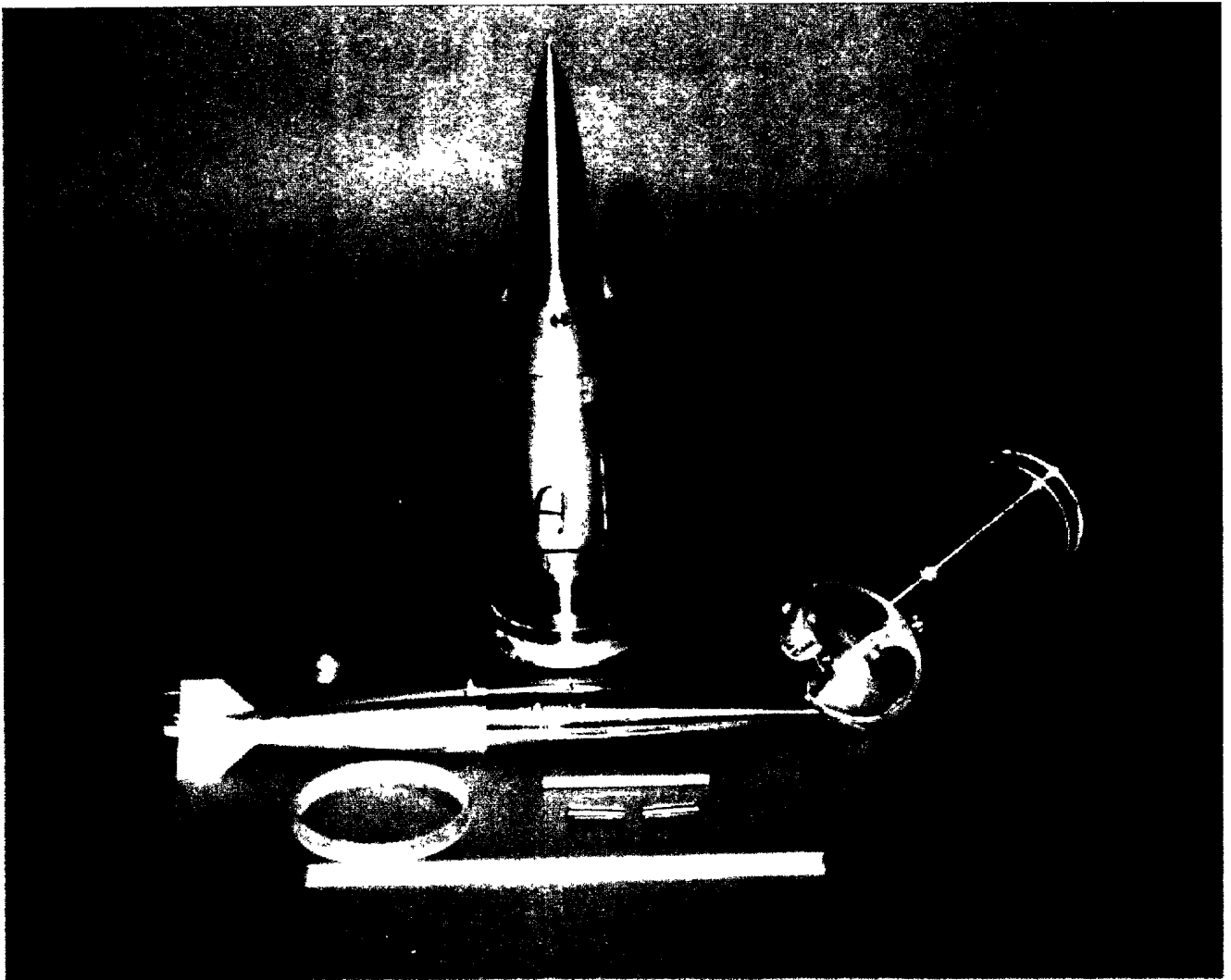


FIGURE 4 - Photograph of model and sabot package of MK-82 configuration

UNCLASSIFIED

FIGURE 5 - DREV aeroballistic range

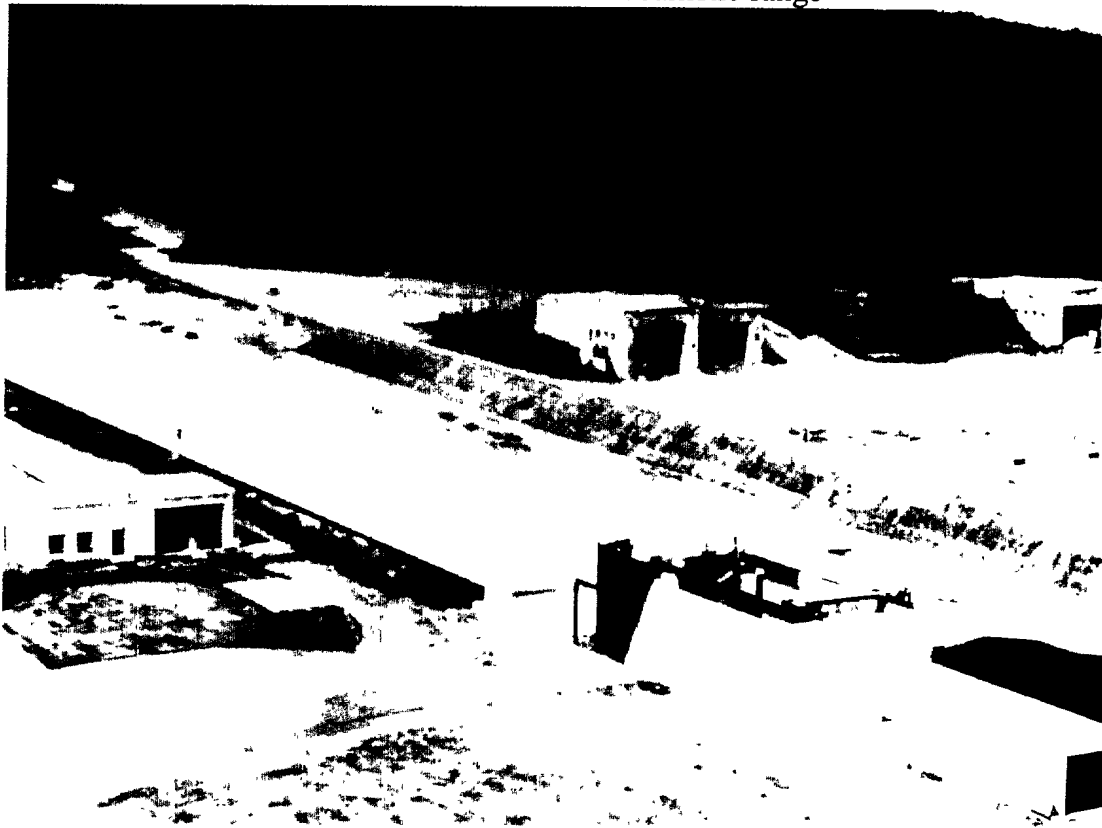


Fig. 5a) Photograph of aeroballistic range complex

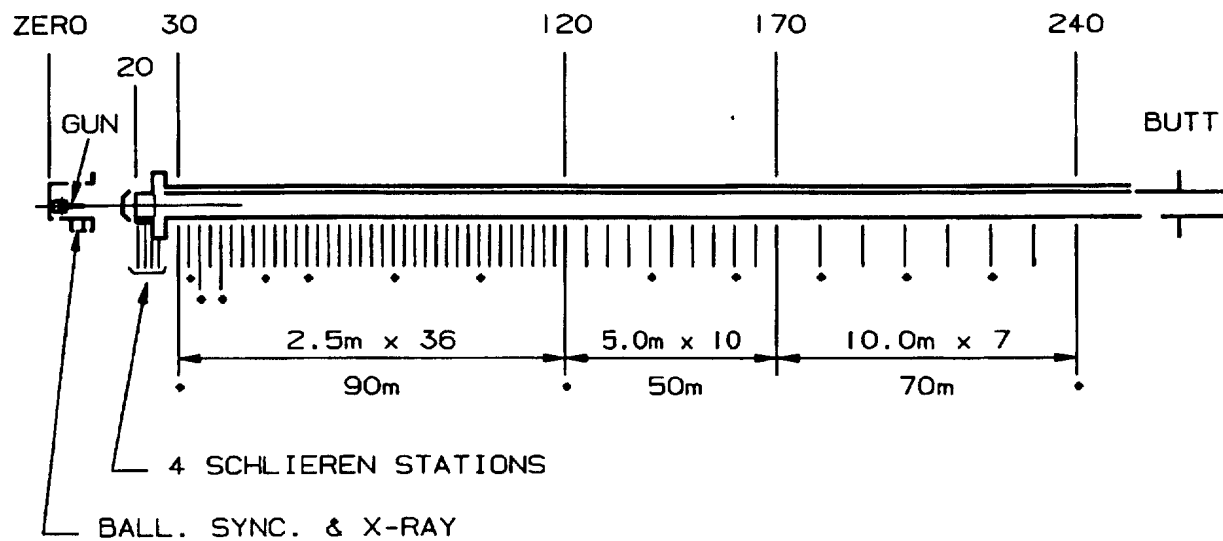


Fig. 5b) Photographic station spacing

UNCLASSIFIED

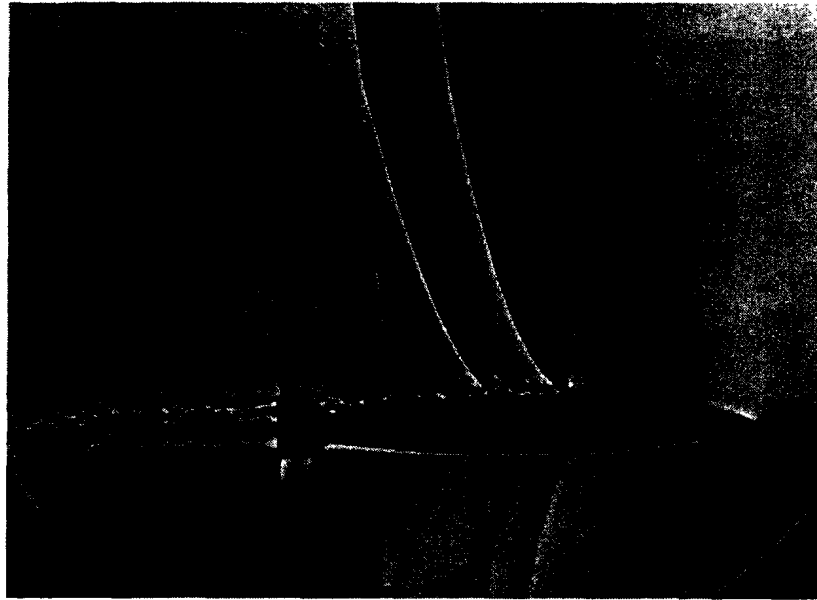


FIGURE 6 - Typical Schlieren photograph for MK82 - Shot C09, $M = 0.98$

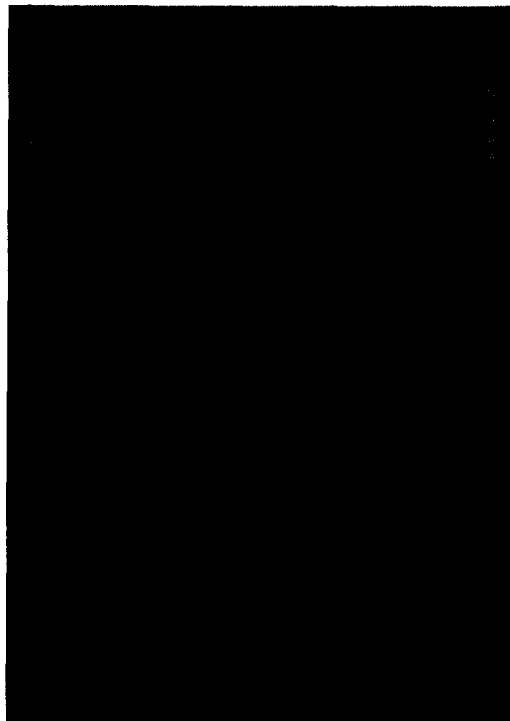


FIGURE 7 - Typical shadowgraph photograph for MK82 - Shot C10, $M = 1.07$

UNCLASSIFIED

ARFDAS - Aeroballistic Range Facility Data Analysis

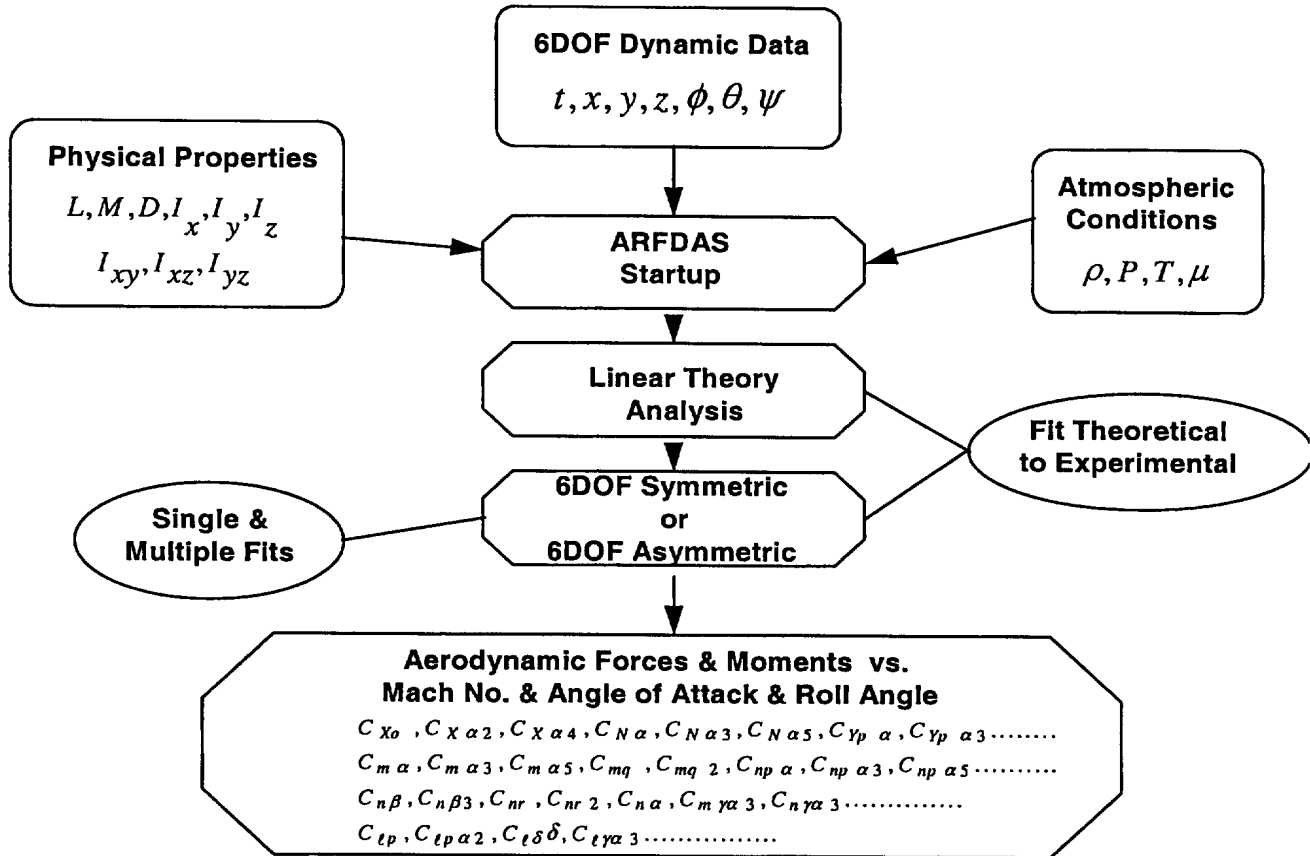


FIGURE 8 - DREV Aeroballistic Range Facility Data Analysis System

UNCLASSIFIED

FIGURE 9 – Comparison of 6DOF reduced aerodynamic coefficients versus Mach number

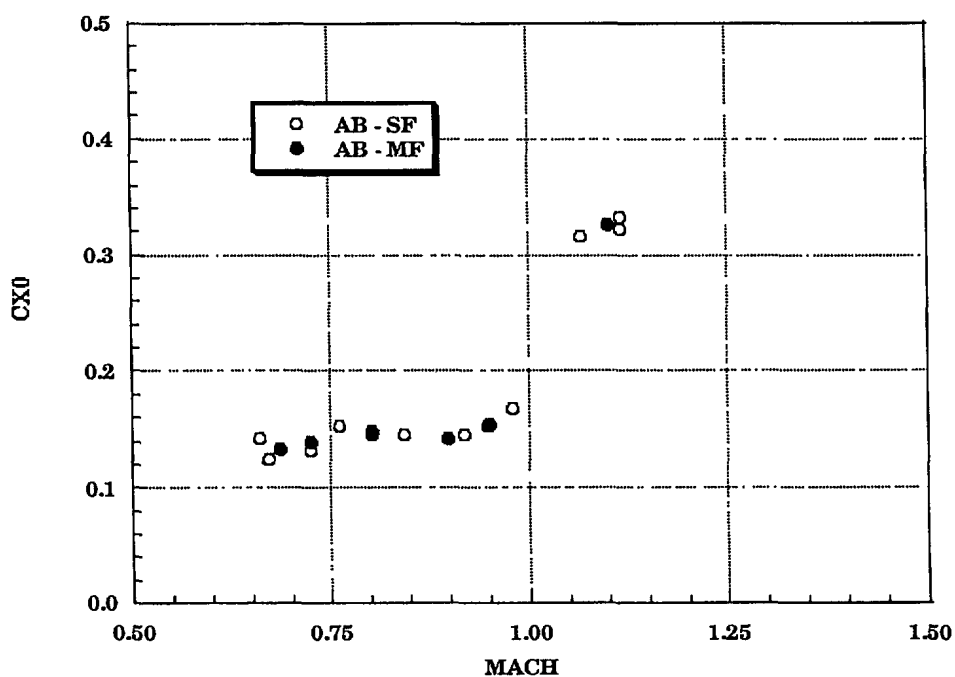


Fig. 9a) Axial force coefficient

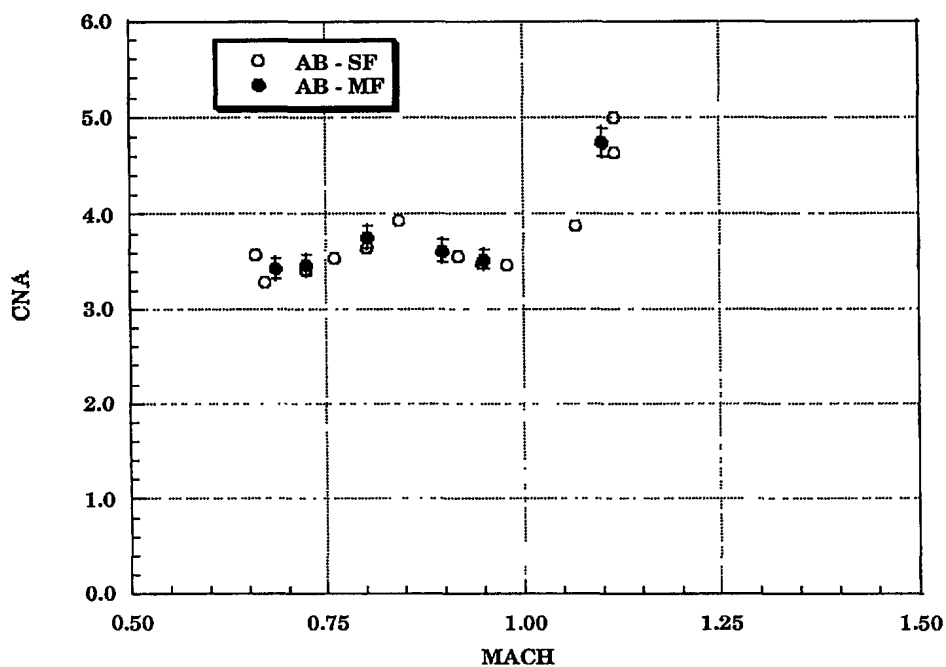


Fig. 9b) Normal force coefficient slope

UNCLASSIFIED

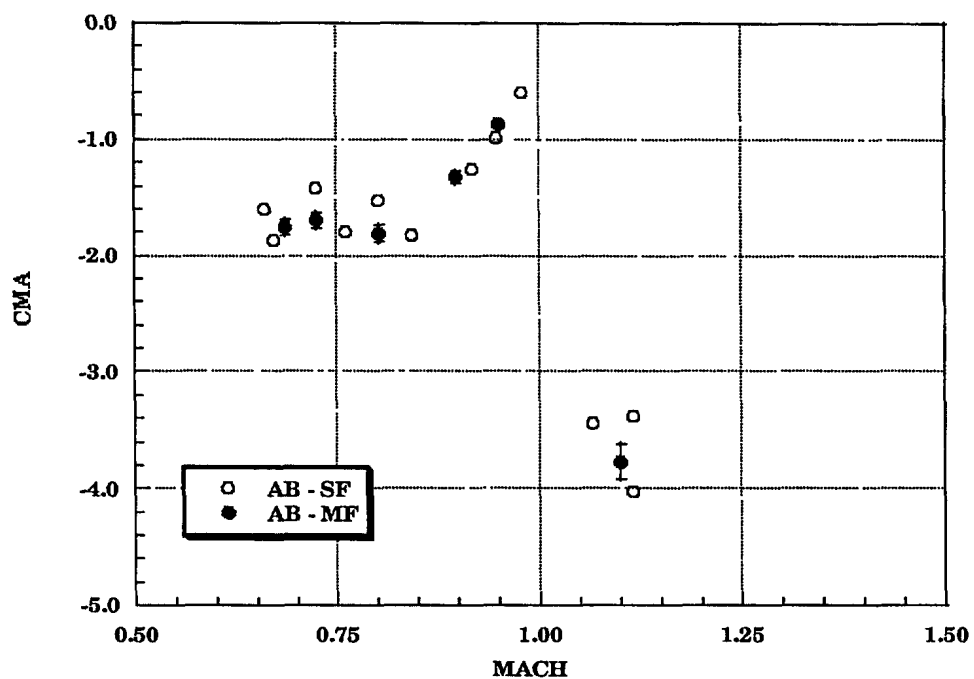


Fig. 9c) Pitch moment coefficient slope

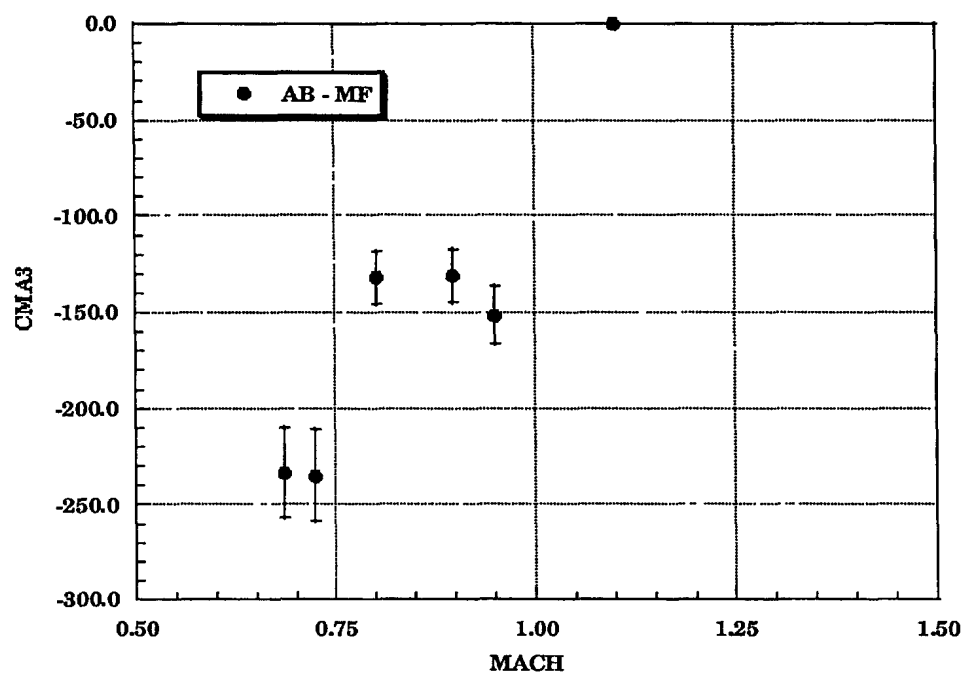


Fig. 9d) Cubic pitch moment coefficient term

UNCLASSIFIED

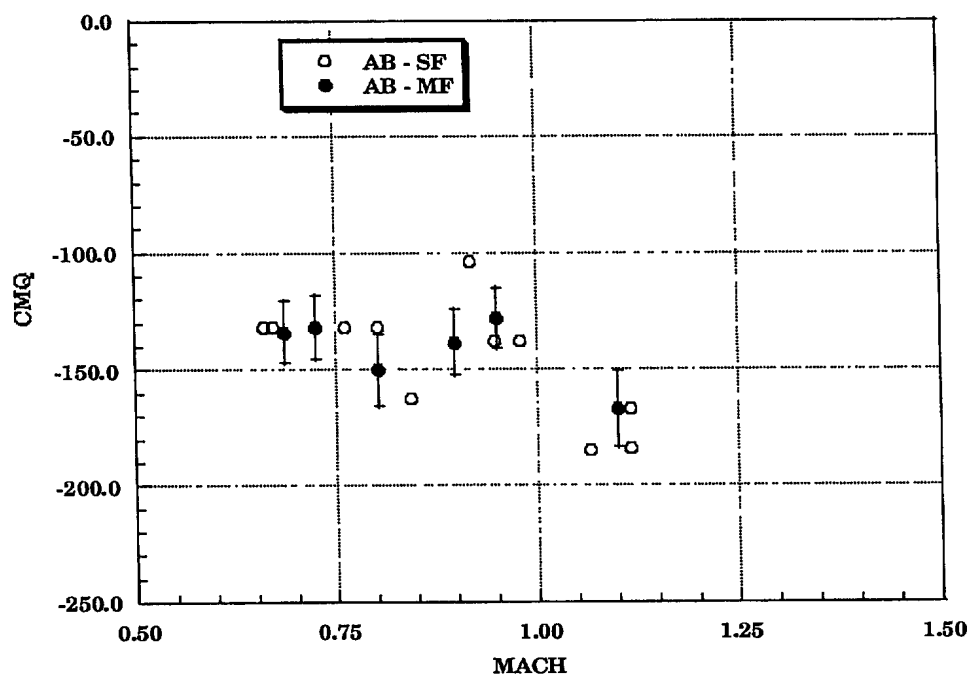


Fig. 9e) Pitch damping coefficient

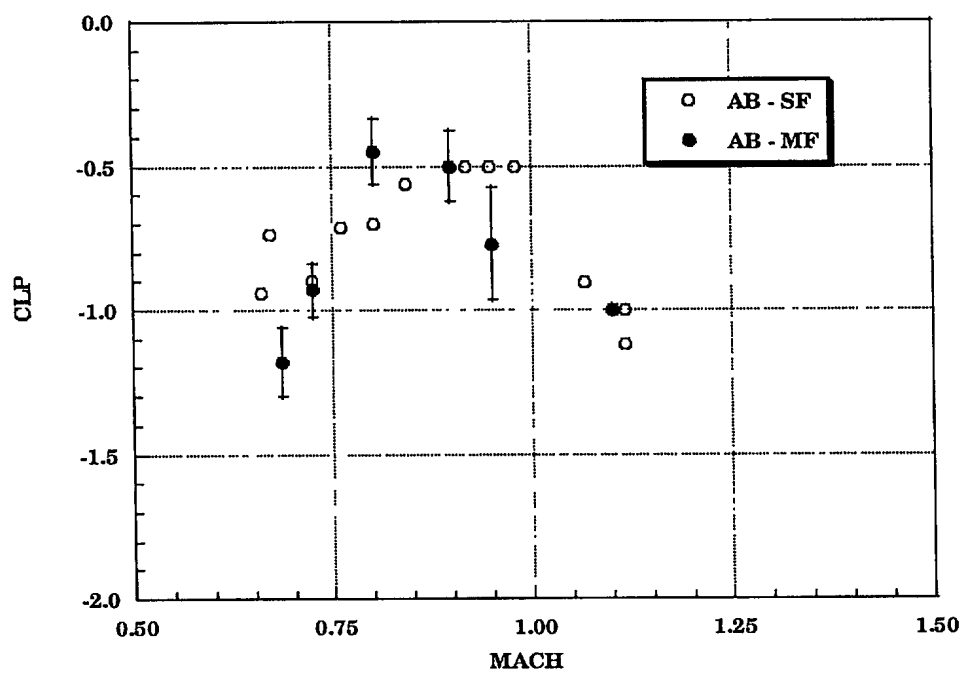


Fig. 9f) Roll damping coefficient

UNCLASSIFIED

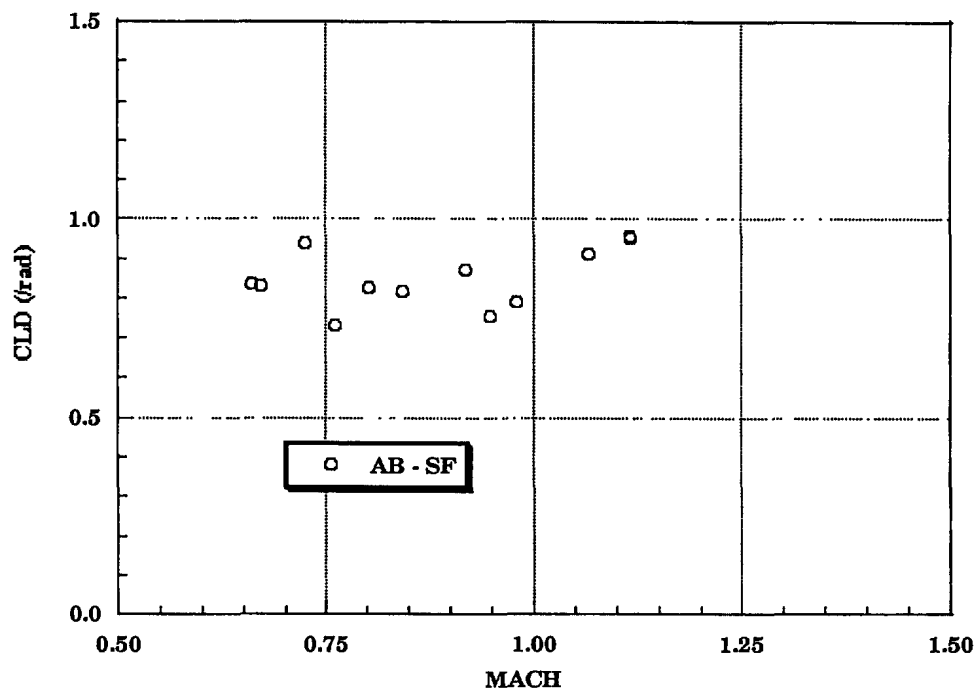


Fig. 9g) Roll moment due to fin cant

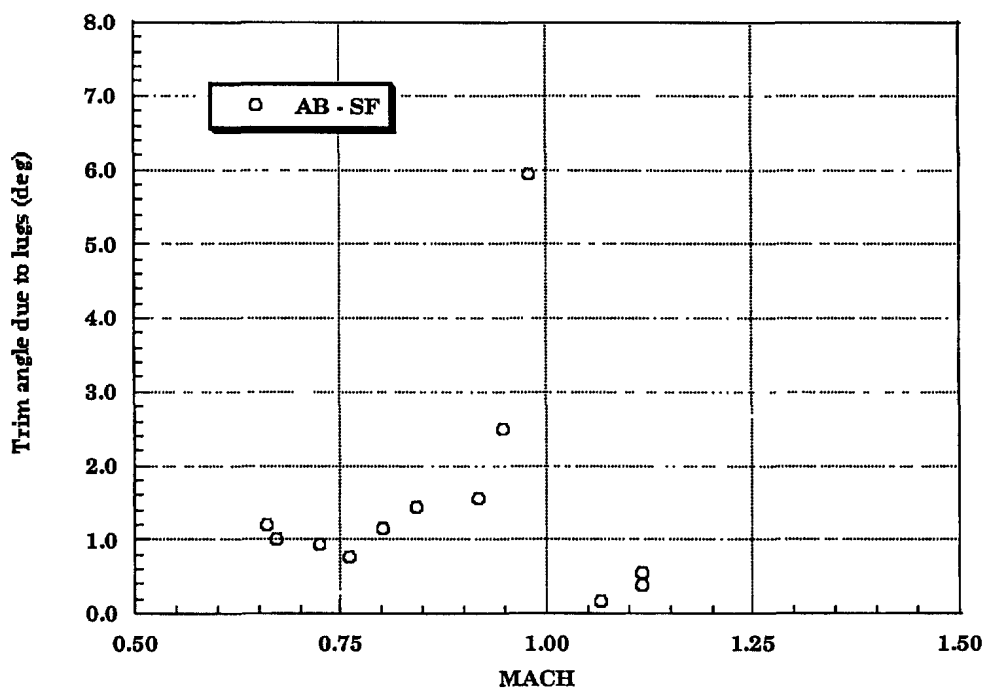


Fig 9h) Trim angle

UNCLASSIFIED

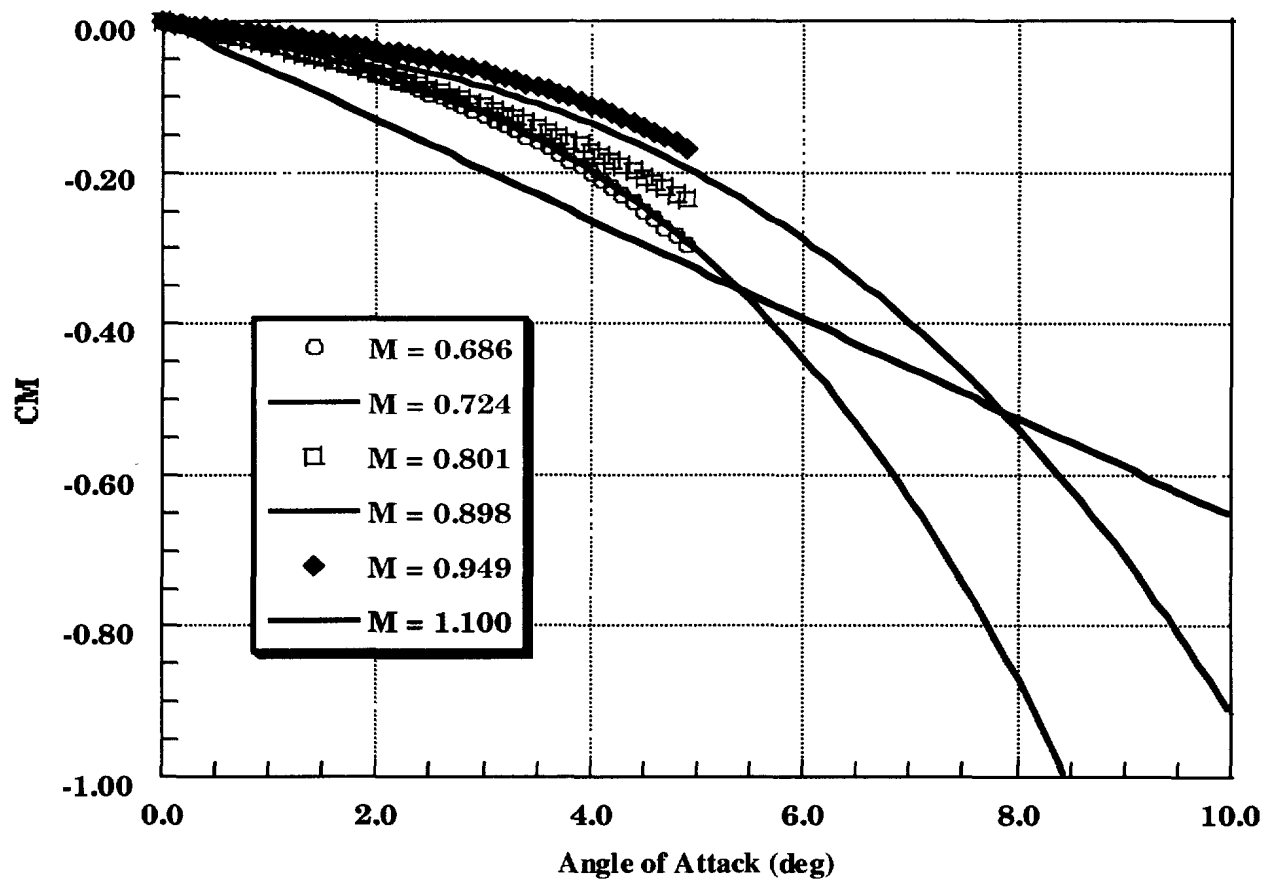


FIGURE 10 – Pitch moment coefficient versus angle of attack

UNCLASSIFIED

FIGURE 11 – Comparison of predicted and experimental results

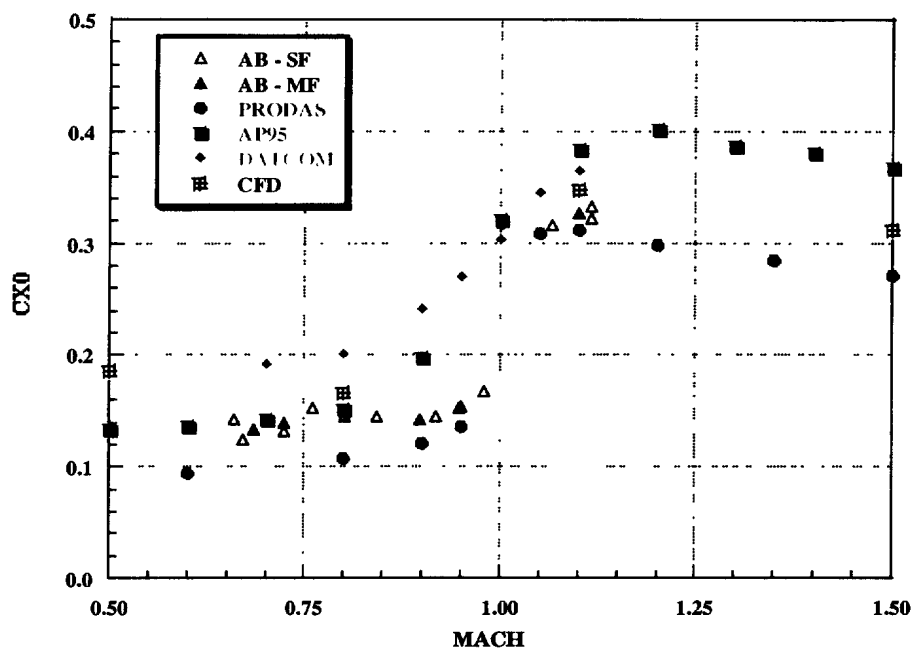


Fig. 11a) Axial force coefficient versus Mach number

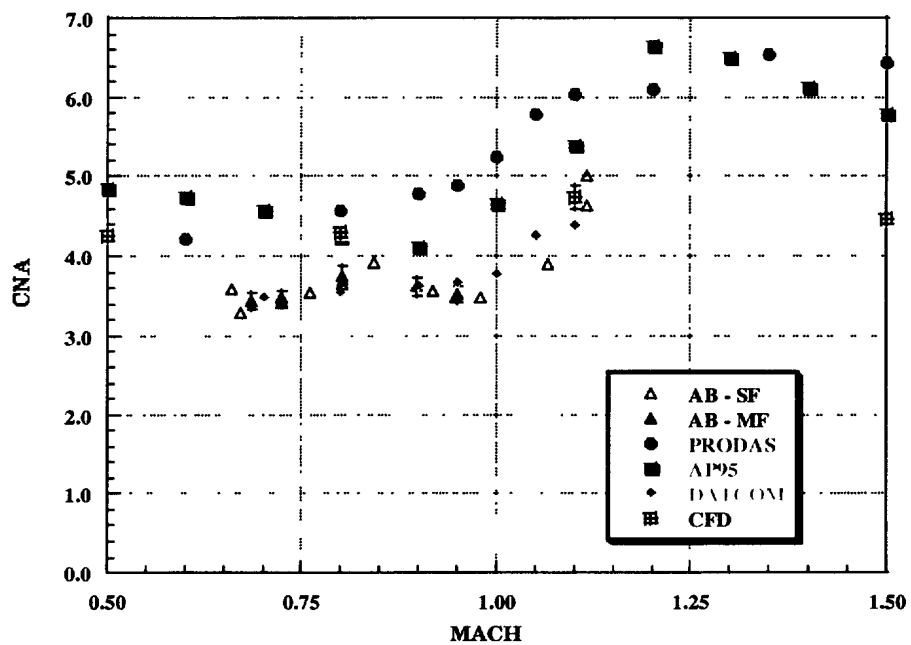


Fig. 11b) Normal force coefficient slope versus Mach number

UNCLASSIFIED

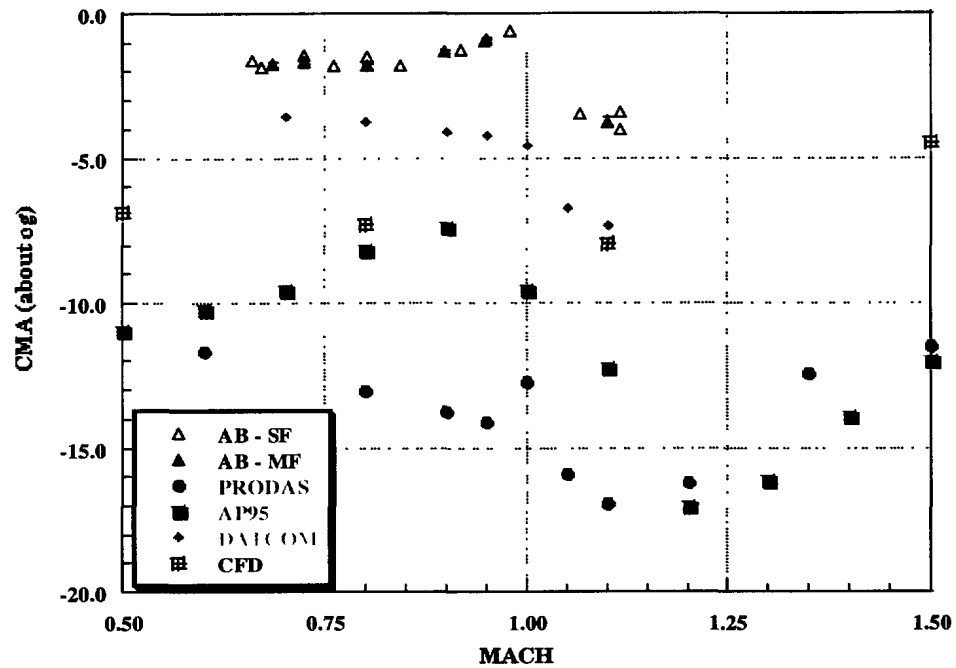


Fig. 11c) Pitch moment coefficient slope versus Mach number

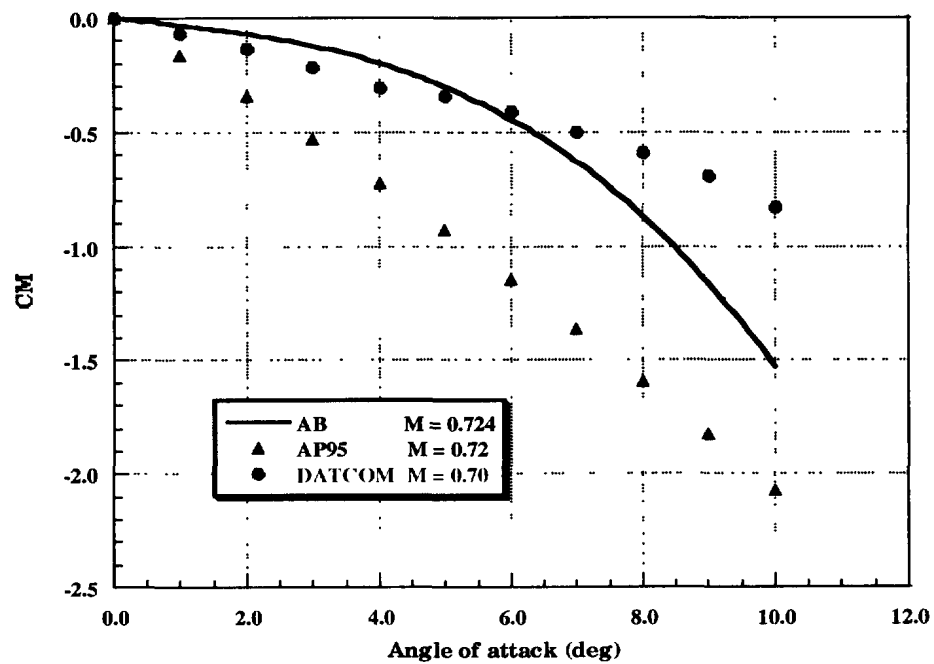


Fig. 11d) Pitch moment coefficient versus angle of attack at Mach 0.72

UNCLASSIFIED

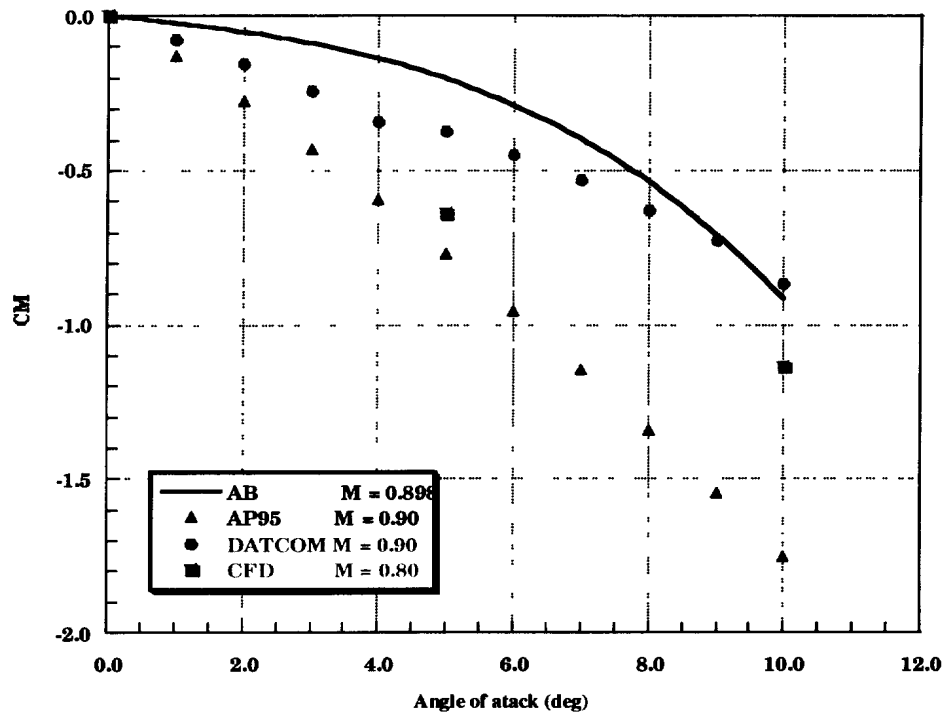


Fig. 11e) Pitch moment coefficient versus angle of attack at Mach 0.90

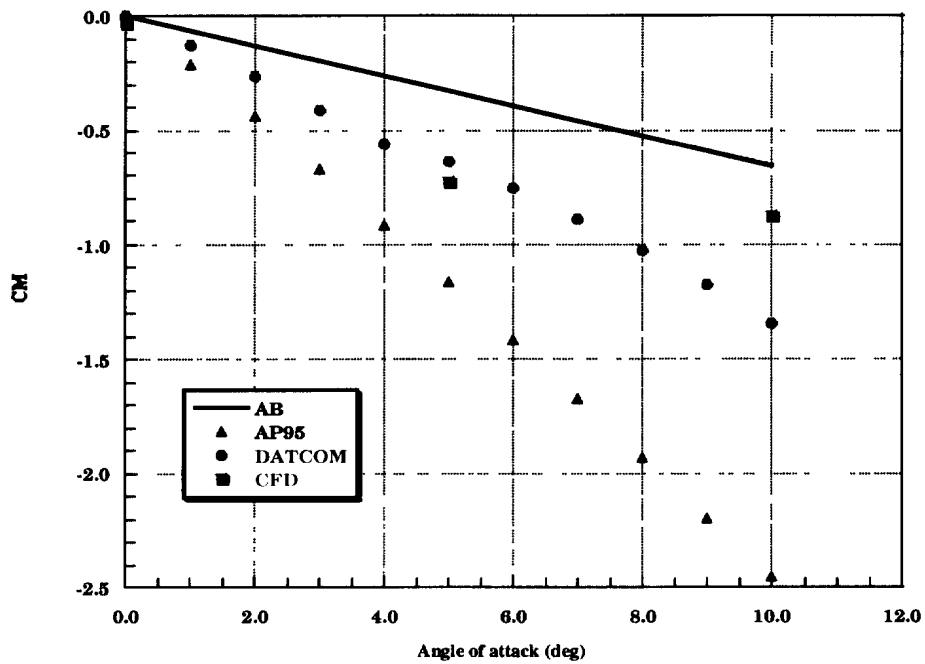


Fig. 11f) Pitch moment coefficient versus angle of attack at Mach 1.10

UNCLASSIFIED

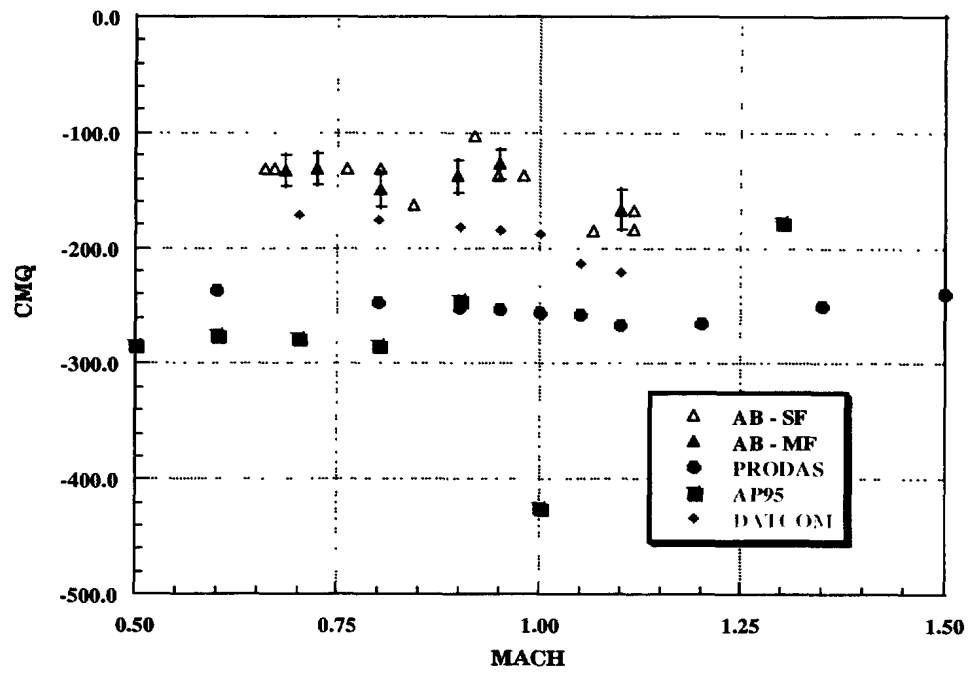


Fig. 11g) Pitch damping coefficient versus Mach number

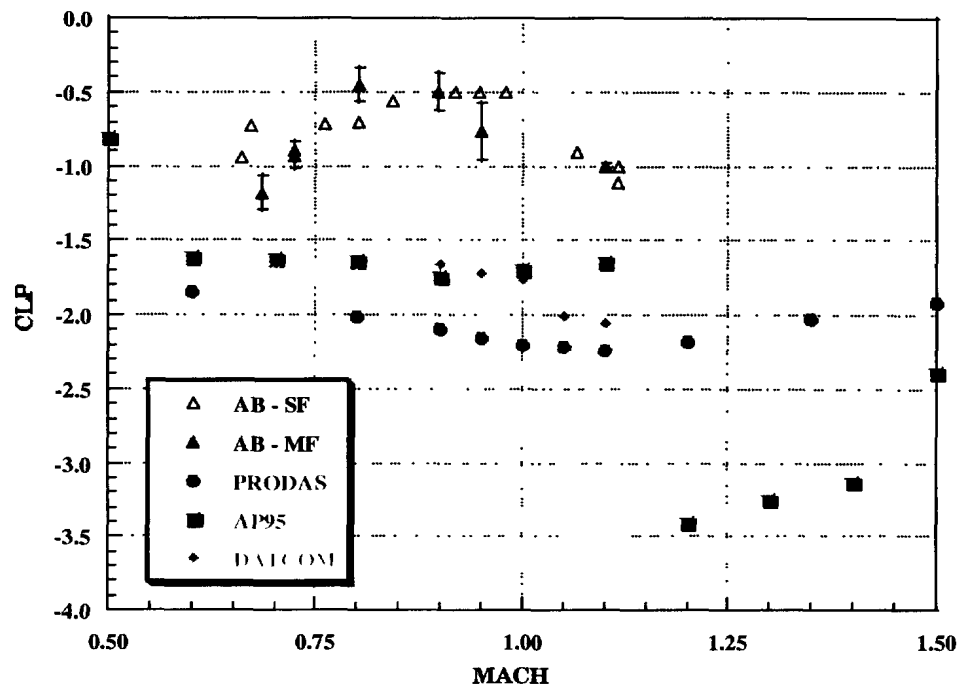


Fig. 11h) Roll damping coefficient versus Mach number

UNCLASSIFIED

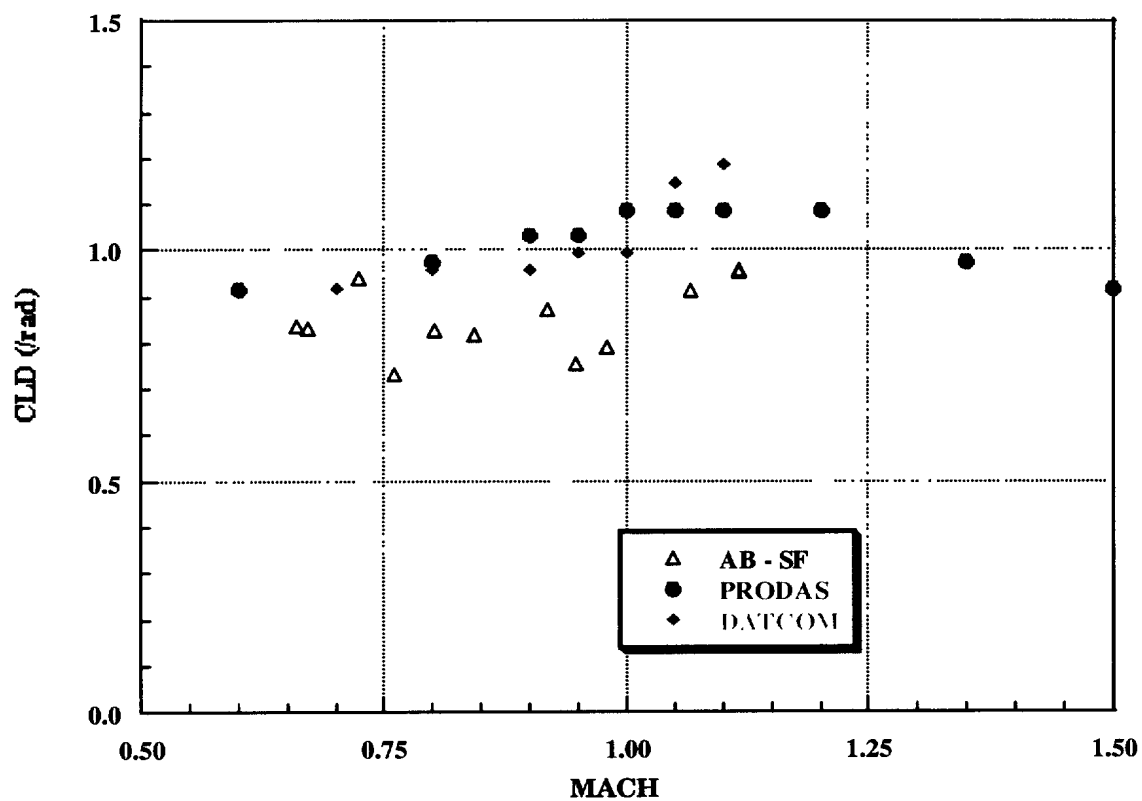


Fig. 11i) Roll moment due to fin cant versus Mach number

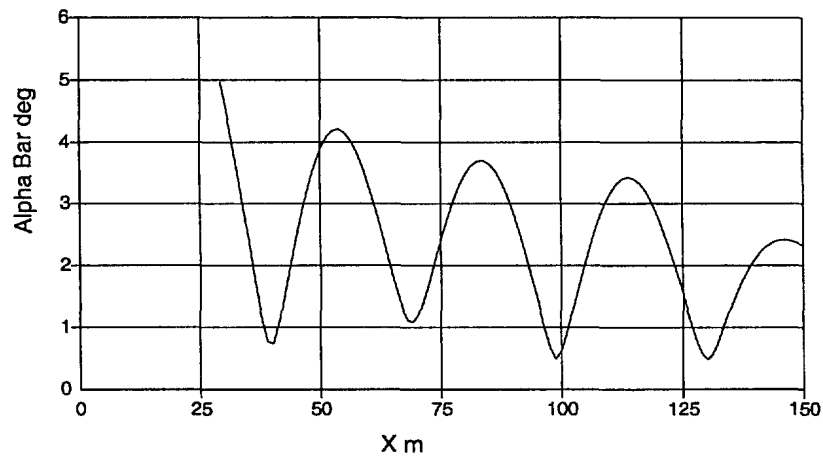
UNCLASSIFIED

APPENDIX A

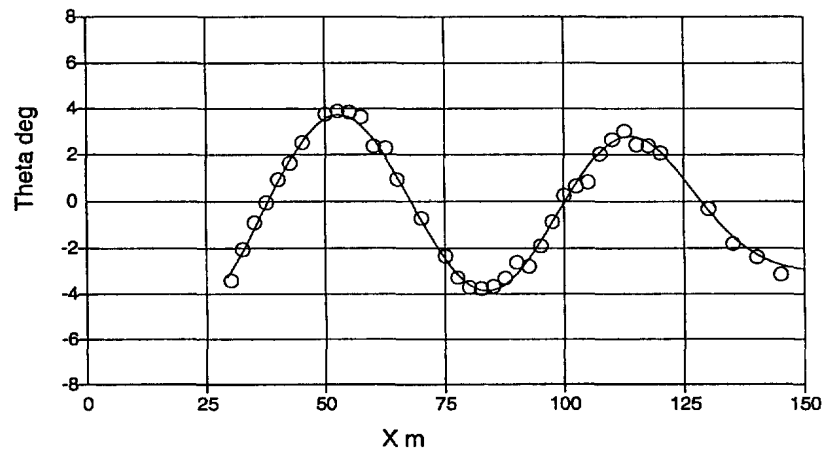
Angular Motion Plots

UNCLASSIFIED

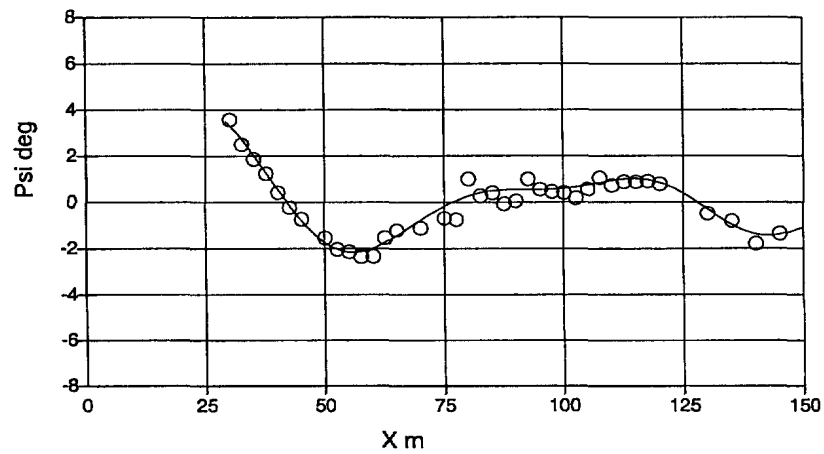
C981001



C981001

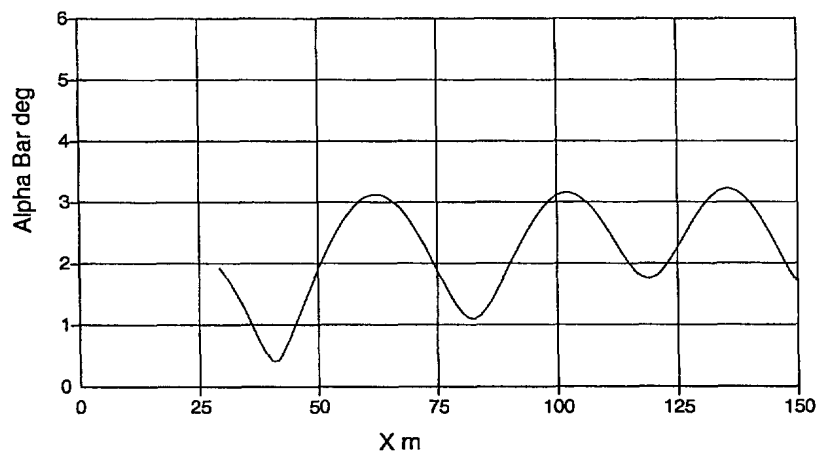


C981001

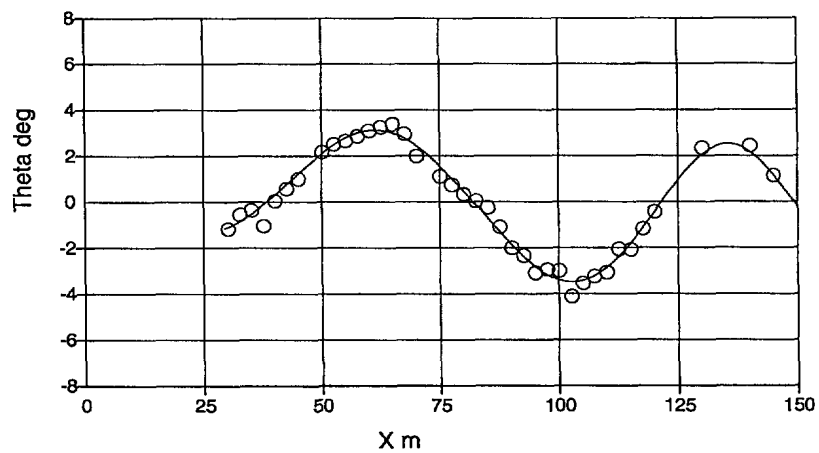


UNCLASSIFIED

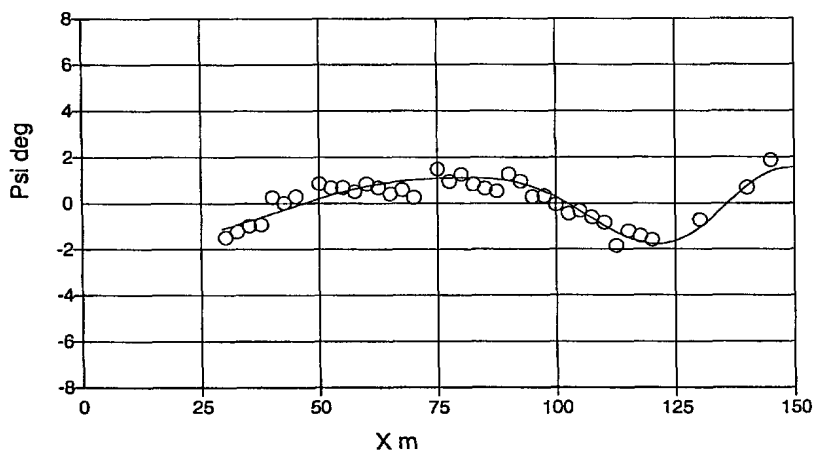
C981002



C981002

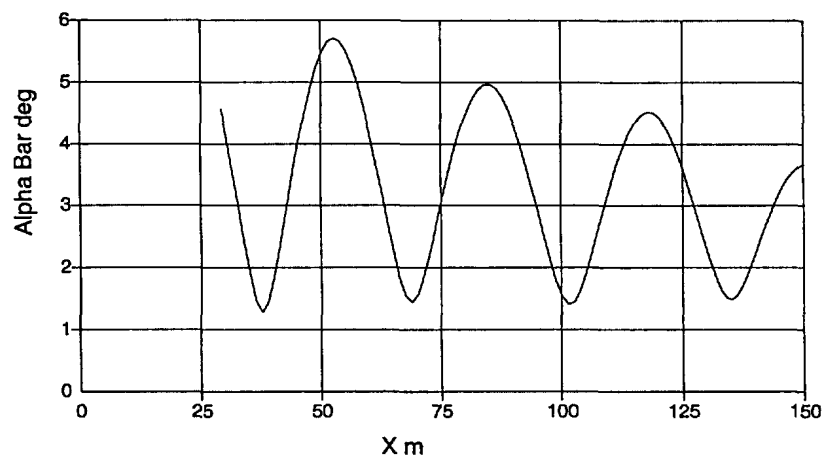


C981002

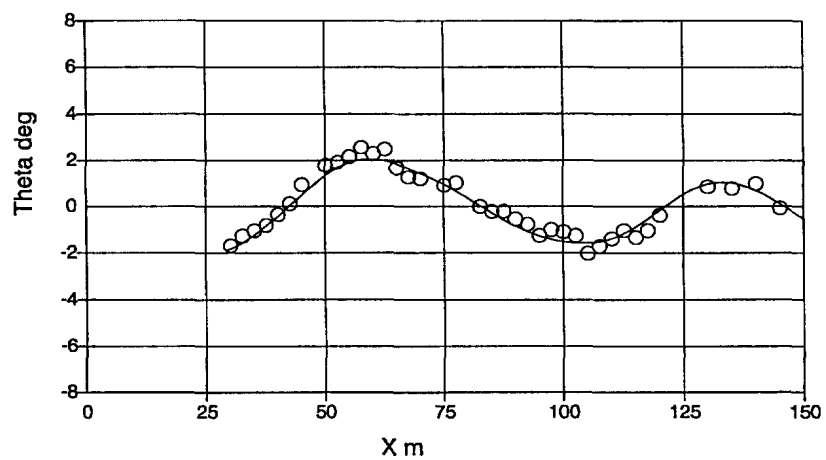


UNCLASSIFIED

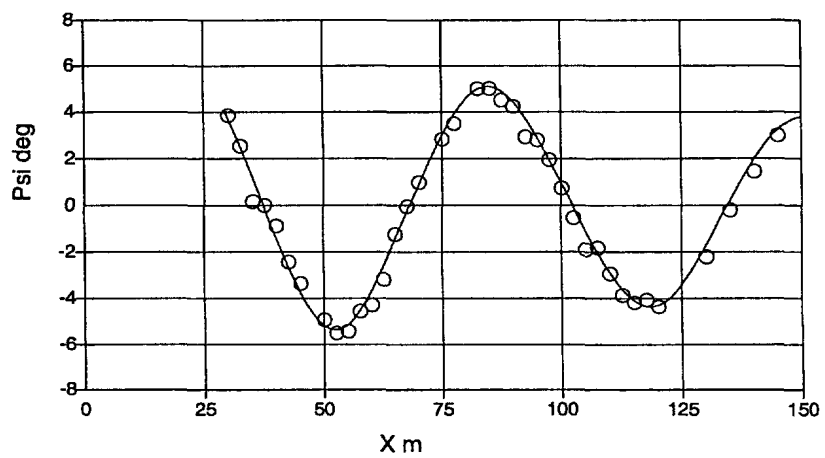
C981003



C981003

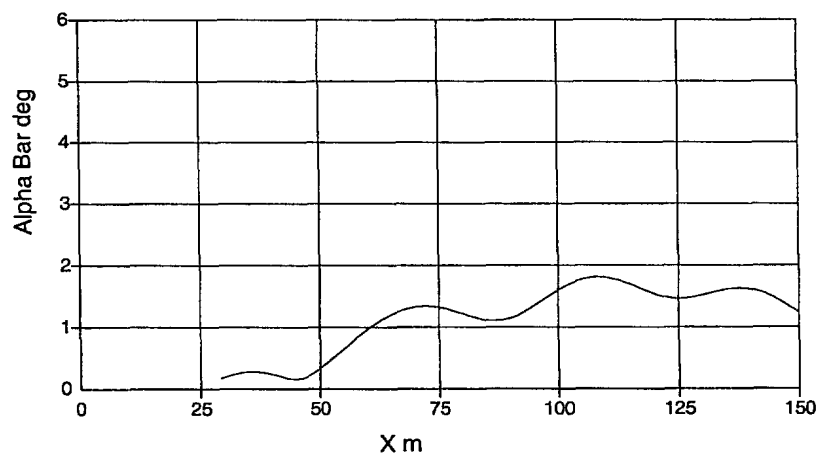


C981003

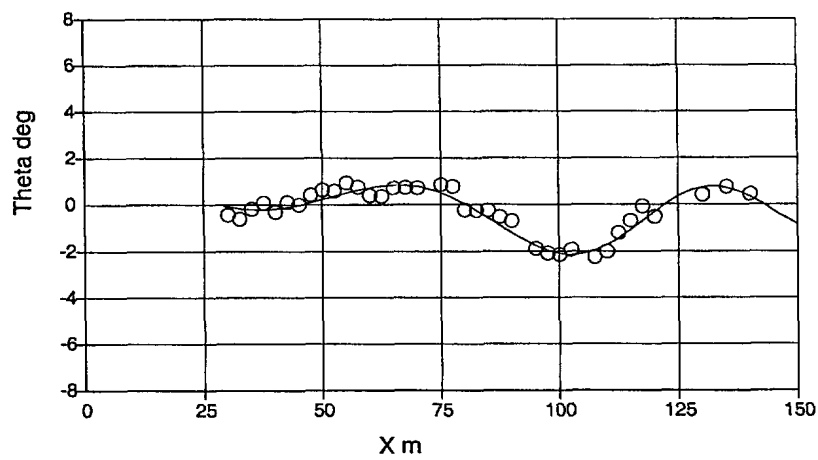


UNCLASSIFIED

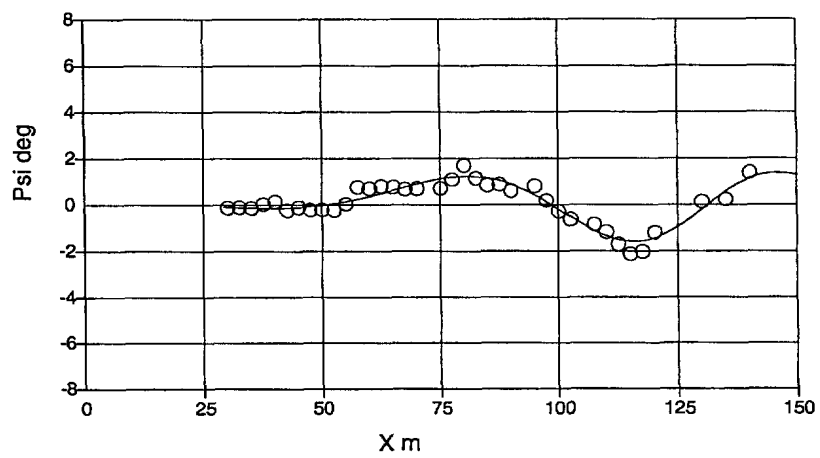
C981004



C981004

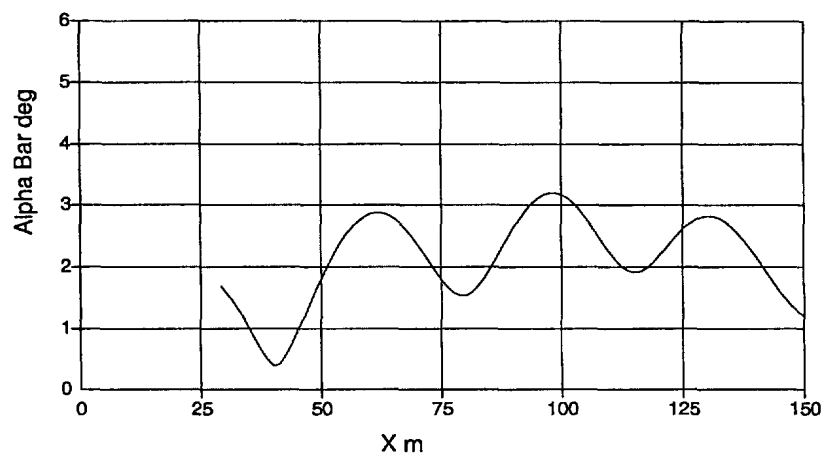


C981004

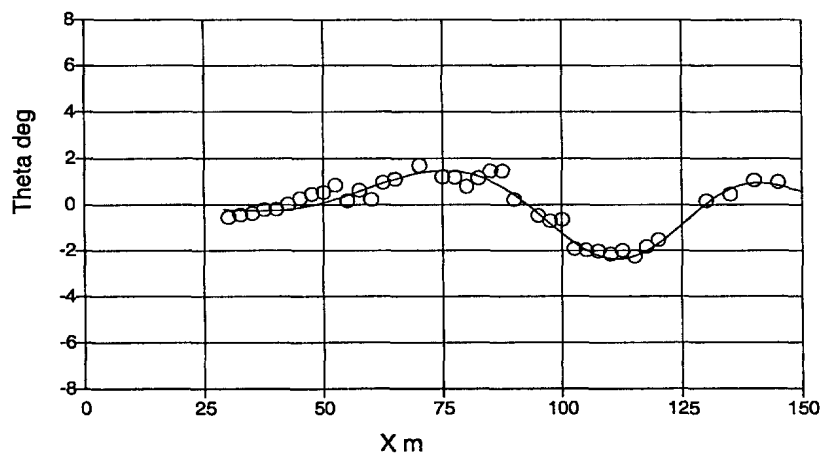


UNCLASSIFIED

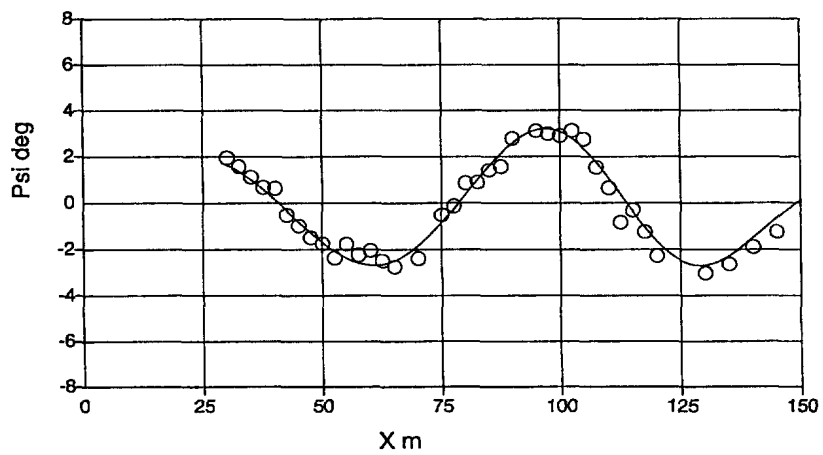
C981005



C981005

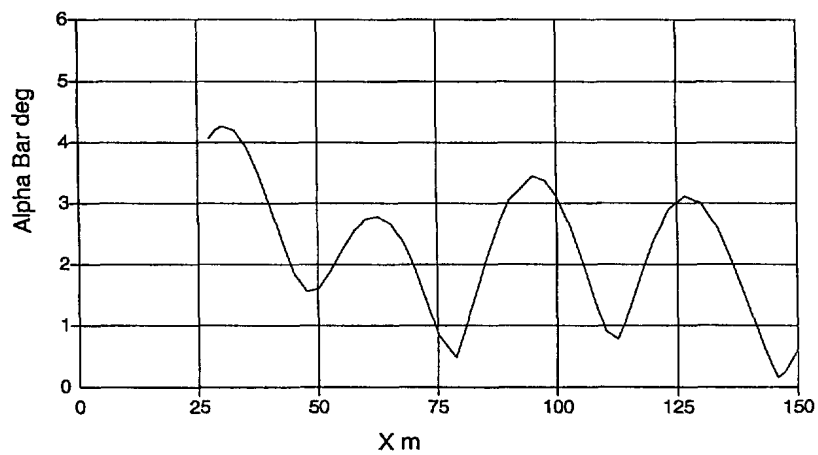


C981005

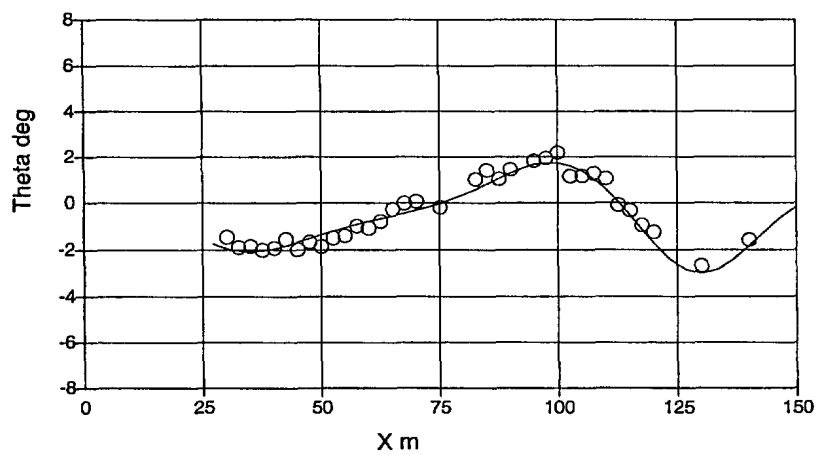


UNCLASSIFIED

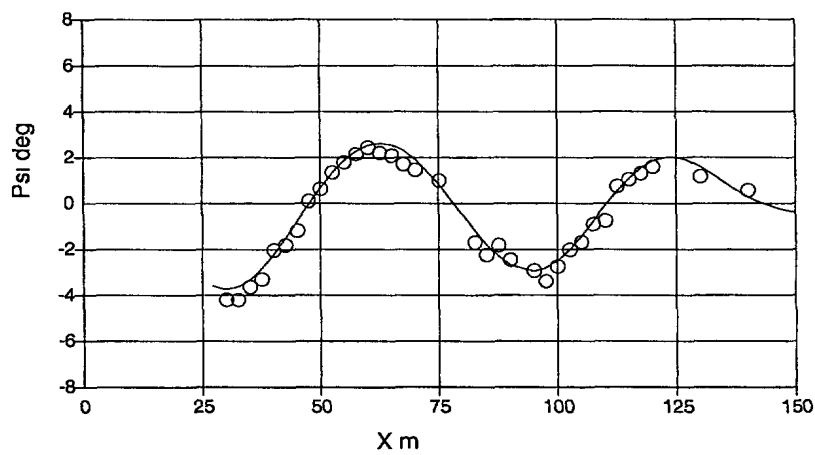
C981006



C981006

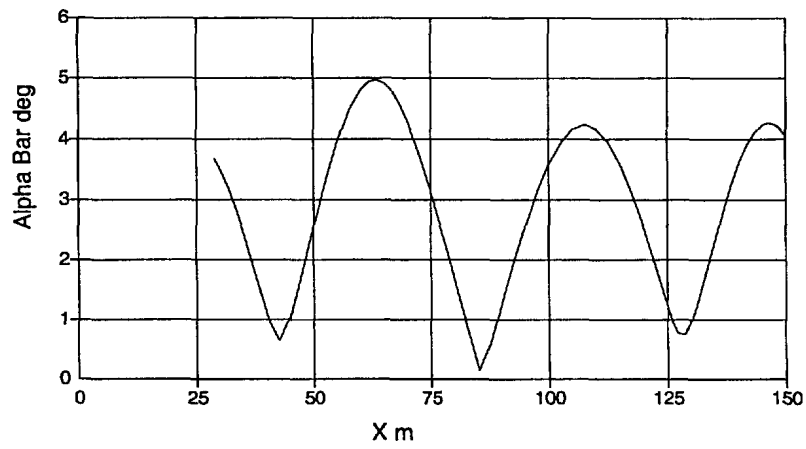


C981006

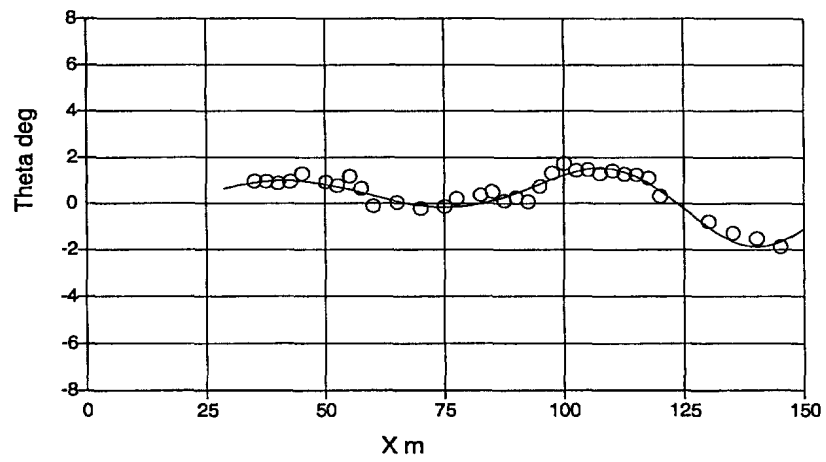


UNCLASSIFIED

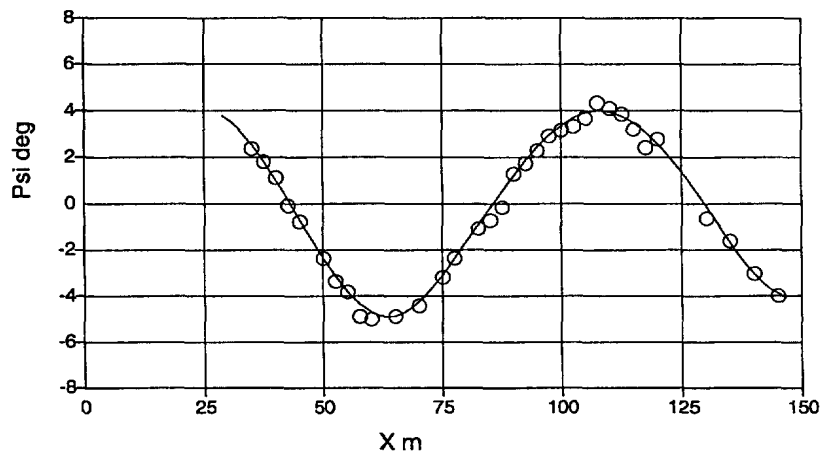
C981007



C981007

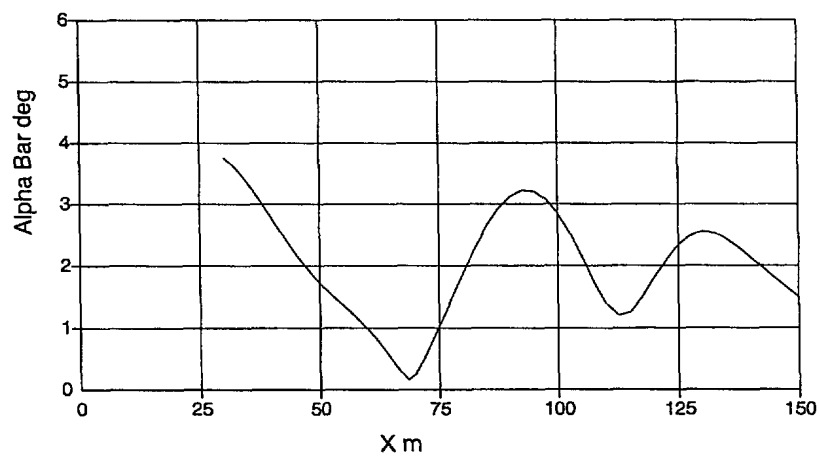


C981007

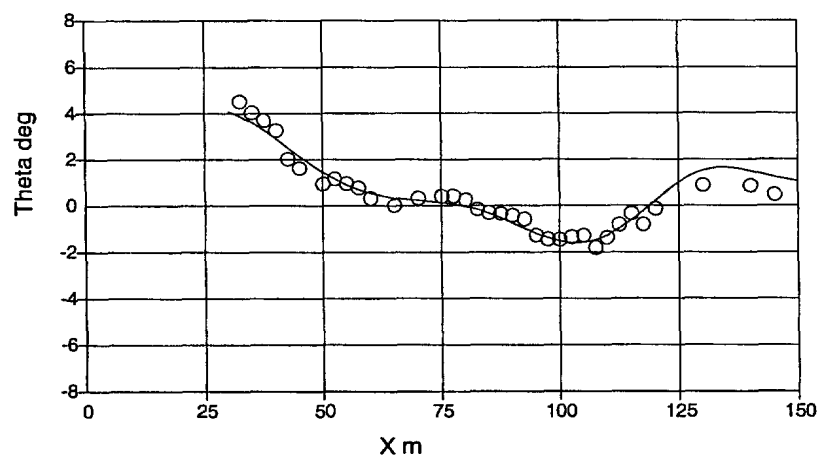


UNCLASSIFIED

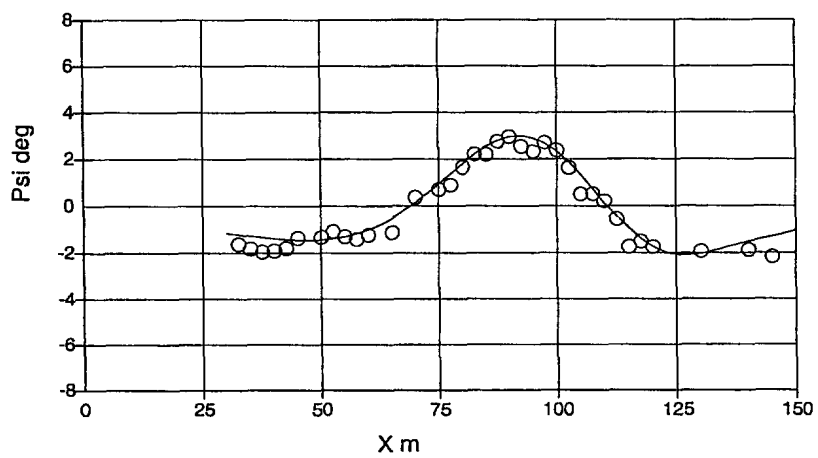
C981008



C981008

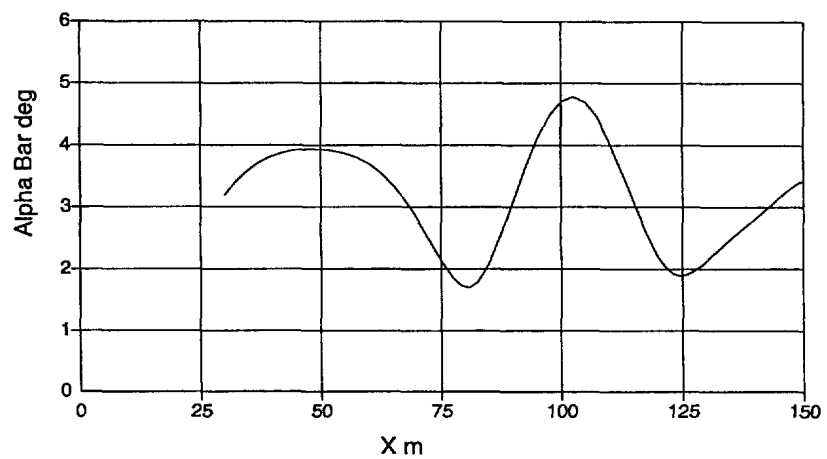


C981008

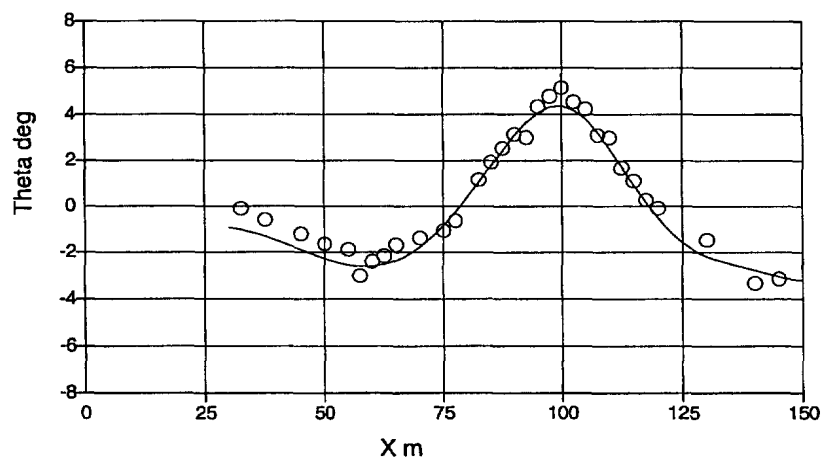


UNCLASSIFIED

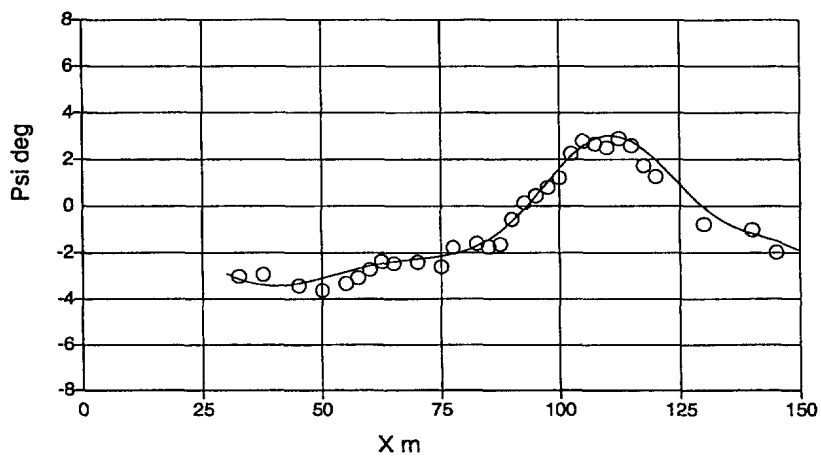
C981009



C981009

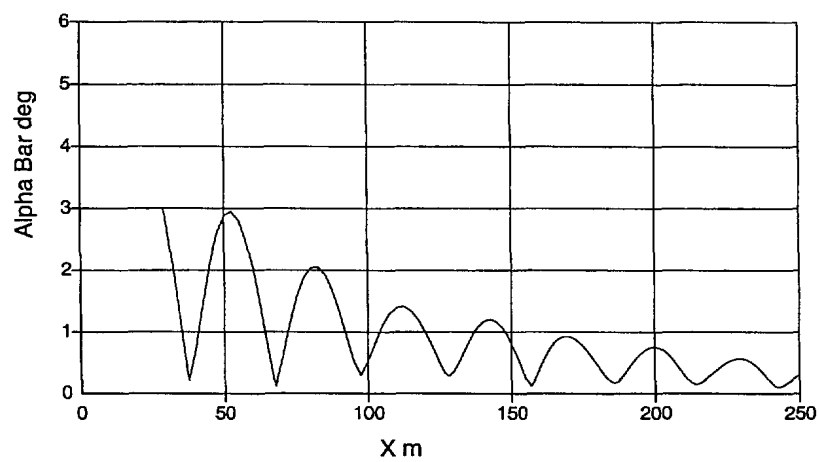


C981009

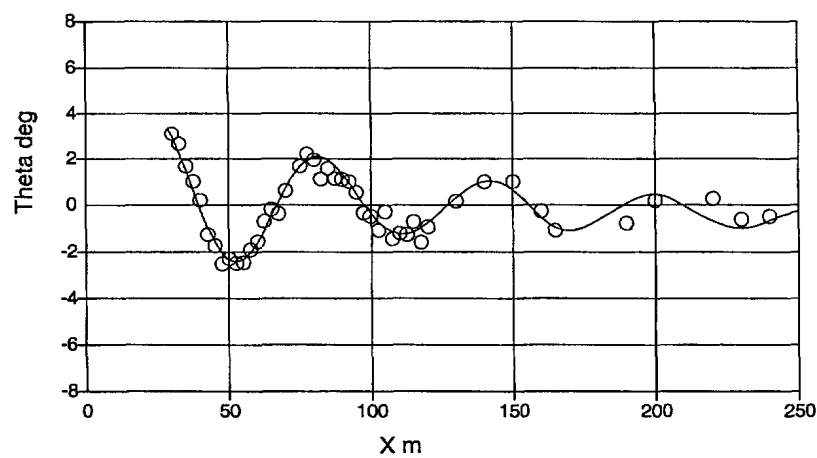


UNCLASSIFIED

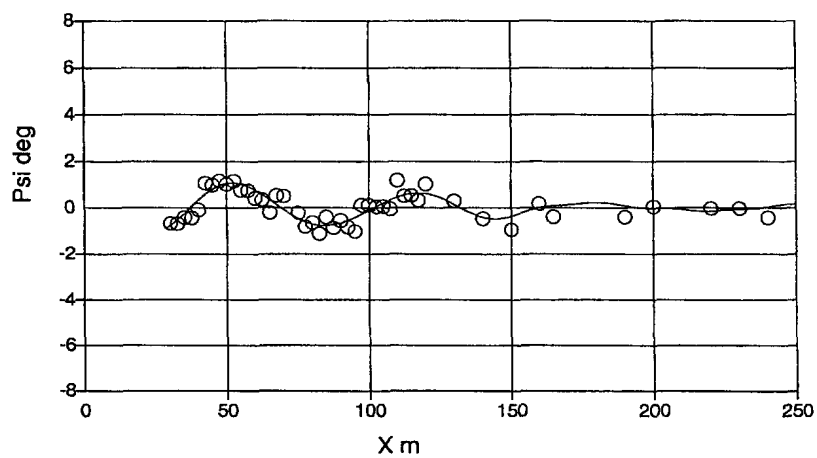
C981110



C981110

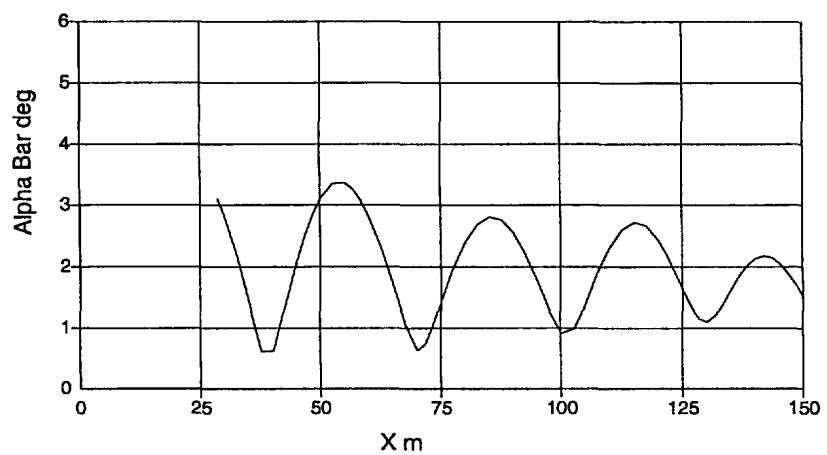


C981110

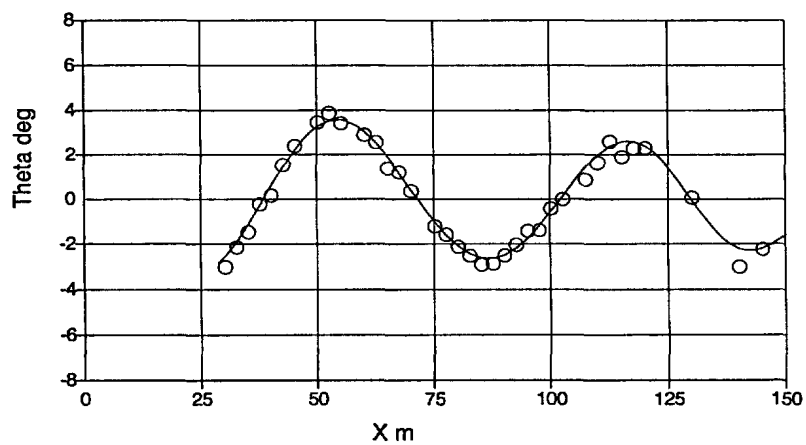


UNCLASSIFIED

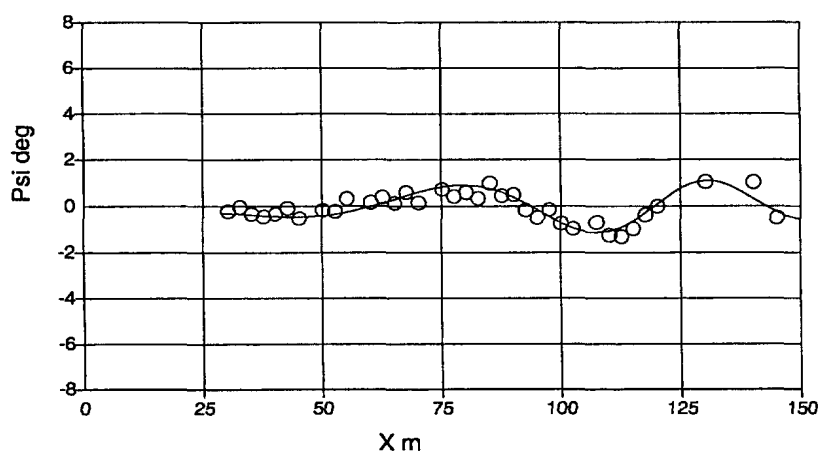
C981011



C981011

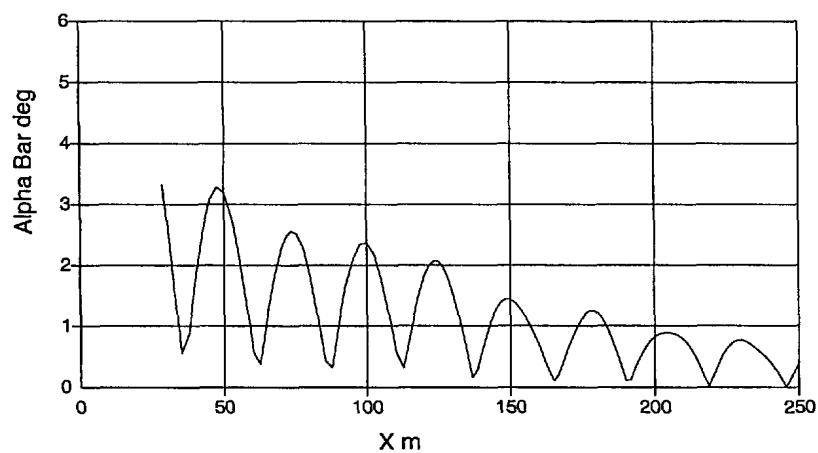


C981011

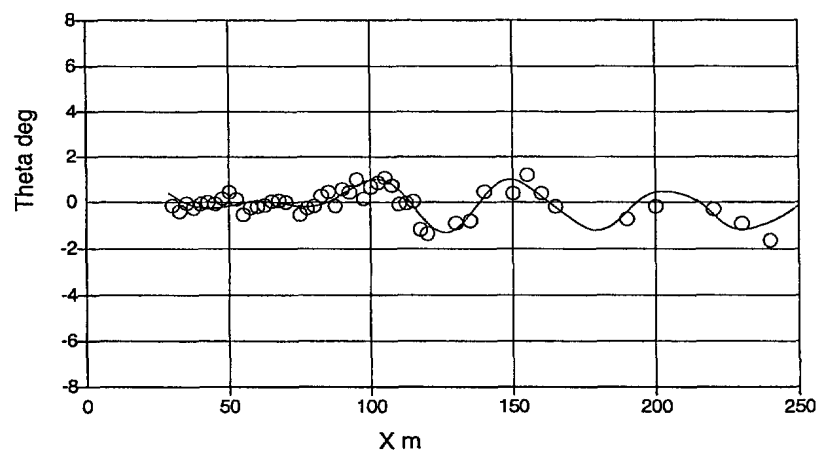


UNCLASSIFIED

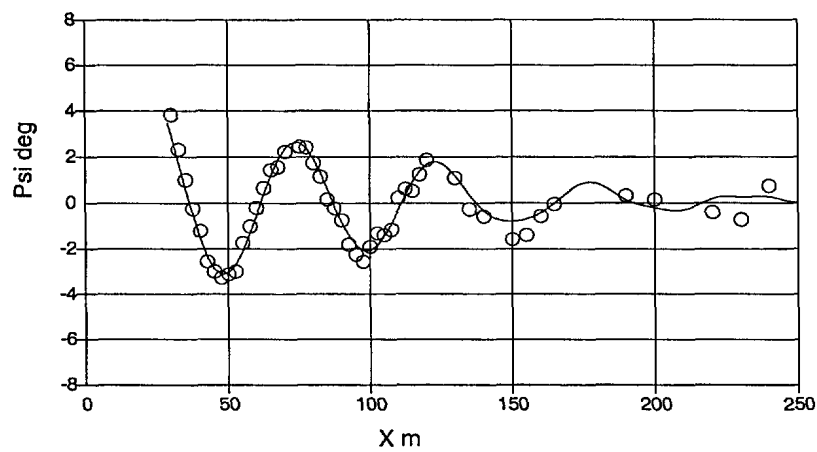
C981112



C981112



C981112



UNCLASSIFIED

INTERNAL DISTRIBUTION

DREV - TM – 2001 - 123

1 – Director General
1 - Deputy Director General
1 - Chief Scientist
6 - Document Library
1 - A. Dupuis (author)
1 - F. Lesage
1 - É. Fournier
1 - A. Jeffrey
1 - G. Dumas
1 - R. Delagrave
1 - M. Lauzon
1 - P. Harris
1 - Maj. Côté
1 - L. Audet
1 – D. Sanschagrín

UNCLASSIFIED

EXTERNAL DISTRIBUTION

DREV - TM – 2001 - 123

1 - DRDKIM
1 - DRDKIM (unbound copy)
1 - DRDC
1 - DSAL
1 - DLR
1 - DAR 5
1 - DNR
1 - DSAA
1 - DSAM
1 - DAEPM (FT) 3
1 - DTA
1 - DTA 3-4
1 - DAPM (ES) 4-3
2 - DRES
1 - CEEM - V
1 - AETE
1 – WSM det Mirabel/SE 6

UNCLASSIFIED

1- Mr. N. Stathopoulos

Dept. 775

Bombardier Aerospace

1800 Marcel Laurin Blvd

St-Laurent, QC

H4R 1K2

1- Mr. N. Tang

High Speed Aerodynamic Laboratory

Institute for Aerospace Research

National Research Council Canada

Montreal Road

Ottawa, Ontario

K1A 0R6

SANS CLASSIFICATION
COTE DE SÉCURITÉ DE LA FORMULE
(plus haut niveau du titre, du résumé ou des mots-clefs)

FICHE DE CONTRÔLE DU DOCUMENT		
1. PROVENANCE (le nom et l'adresse) CRDV	2. COTE DE SÉCURITÉ (y compris les notices d'avertissement, s'il y a lieu) UNCLASSIFIED	
3. TITRE (Indiquer la cote de sécurité au moyen de l'abréviation (S, C, R ou U) mise entre parenthèses, immédiatement après le titre.) FREE-FLIGHT AERODYNAMIC CHARACTERISTIC OF THE LDGP MK-82 CF BOMB AT SUBSONIC AND TRANSONIC VELOCITIES		
4. AUTEURS (Nom de famille, prénom et initiales. Indiquer les grades militaires, ex.: Bieau, Maj. Louis E.) A. Dupuis		
5. DATE DE PUBLICATION DU DOCUMENT (mois et année) Septembre 2001	6a. NOMBRE DE PAGES 100	6b. NOMBRE DE REFERENCES 15
7. DESCRIPTION DU DOCUMENT (La catégorie du document, par exemple rapport, note technique ou memorandum. Indiquer les dates lorsque le rapport couvre une période définie.) DREV TM		
8. PARRAIN (le nom et l'adresse) NDHQ DTA		
9a. NUMÉRO DU PROJET OU DE LA SUBVENTION (Spécifier si c'est un projet ou une subvention) 3ec16	9b. NUMÉRO DE CONTRAT	
10a. NUMÉRO DU DOCUMENT DE L'ORGANISME EXPÉDITEUR	10b. AUTRES NUMÉROS DU DOCUMENT <div style="text-align: center;">N/A</div>	
11. ACCÈS AU DOCUMENT (Toutes les restrictions concernant une diffusion plus ample du document, autres que celles inhérentes à la cote de sécurité.) <div style="display: flex; margin-top: 5px;"> <div style="margin-right: 10px;"> <input checked="" type="checkbox"/> <input type="checkbox"/> <input type="checkbox"/> <input type="checkbox"/> <input type="checkbox"/> <input type="checkbox"/> </div> <div> Diffusion illimitée Diffusion limitée aux entrepreneurs des pays suivants (spécifier) Diffusion limitée aux entrepreneurs canadiens (avec une justification) Diffusion limitée aux organismes gouvernementaux (avec une justification) Diffusion limitée aux ministères de la Défense Autres (préciser) </div> </div>		
12. ANNONCE DU DOCUMENT (Toutes les restrictions à l'annonce bibliographique de ce document. Cela correspond, en principe, aux données d'accès au document (11). Lorsqu'une diffusion supplémentaire (à d'autres organismes que ceux précisés à la case 11) est possible, on pourra élargir le cercle de diffusion de l'annonce.) illimitée		

SANS CLASSIFICATION
COTE DE LA SÉCURITÉ DE LA FORMULE
(plus haut niveau du titre, du résumé ou des mots-clefs)

SANS CLASSIFICATION

COTE DE LA SÉCURITÉ DE LA FORMULE

(plus haut niveau du titre, du résumé ou des mots-clefs)

13. SOMMAIRE (Un résumé clair et concis du document. Les renseignements peuvent aussi figurer ailleurs dans le document. Il est souhaitable que le sommaire des documents classifiés soit non classifié. Il faut inscrire au commencement de chaque paragraphe du sommaire la cote de sécurité applicable aux renseignements qui s'y trouvent, à moins que le document lui-même soit non classifié. Se servir des lettres suivantes: (S), (C), (R) ou (U). Il n'est pas nécessaire de fournir ici des sommaires dans les deux langues officielles à moins que le document soit bilingue.)

Free-flight tests were conducted in the Defence Research Establishment Valcartier (DREV) aeroballistic range on a 18.6% scaled model of the Low Drag General Purpose (LDGP) MK82 CF (Conical Fin) bomb from subsonic to low supersonic velocities. All the main aerodynamic coefficients and dynamic stability derivatives as well as nonlinear ones were determined using the six-degree-of-freedom single- and multiple-fit data reduction techniques. The pitch moment coefficient was highly nonlinear at low angles of attack in the subsonic and transonic regime. Estimates of the aerodynamic coefficients from three analytical codes and from one computational fluid dynamic analyses were compared with the free-flight results.

516270
CA011719

14. MOTS-CLÉS, DESCRIPTEURS OU RENSEIGNEMENTS SPÉCIAUX (Expressions ou mots significatifs du point de vue technique, qui caractérisent un document et peuvent aider à le cataloguer. Il faut choisir des termes qui n'exigent pas de cote de sécurité. Des renseignements tels que le modèle de l'équipement, la marque de fabrique, le nom de code du projet militaire, la situation géographique, peuvent servir de mots-clés. Si possible, on doit choisir des mots-clés d'un thésaurus, par exemple le "Thesaurus of Engineering and Scientific Terms (TESTS)". Nommer ce thésaurus. Si l'on ne peut pas trouver de termes non classifiés, il faut indiquer la classification de chaque terme comme on le fait avec le titre.)

FREE-FLIGHT TESTS

PROJECTILE DESIGN

MK82

AERODYNAMIC COEFFICIENTS

6DOF

MLM METHODOLOGY

AEROBALLISTIC RANGE TESTS

LINEAR THEORY

BOMBS

MK-82 LDGP

GUN LAUNCHED

SUBSONIC

TRANSONIC

FINNED PROJECTILE

FLIGHT DYNAMICS

STABILITY

SANS CLASSIFICATION

COTE DE SÉCURITÉ DE LA FORMULE

(plus haut niveau du titre, du résumé ou des mots-clefs)